

RETRAN-3D Analysis of BWR Control Rod Drop Accidents



WARNING:

Please read the Export Control Agreement on the back cover.

Effective December 6, 2006, this report has been made publicly available in accordance with Section 734.3(b)(3) and published in accordance with Section 734.7 of the U.S. Export Administration Regulations. As a result of this publication, this report is subject to only copyright protection and does not require any license agreement from EPRI. This notice supersedes the export control restrictions and any proprietary licensed material notices embedded in the document prior to publication.

RETRAN-3D Analysis of BWR Control Rod Drop Accidents

1015206

Final Report, June 2007

EPRI Project Manager
O. Ozer

DISCLAIMER OF WARRANTIES AND LIMITATION OF LIABILITIES

THIS DOCUMENT WAS PREPARED BY THE ORGANIZATION(S) NAMED BELOW AS AN ACCOUNT OF WORK SPONSORED OR COSPONSORED BY THE ELECTRIC POWER RESEARCH INSTITUTE, INC. (EPRI). NEITHER EPRI, ANY MEMBER OF EPRI, ANY COSPONSOR, THE ORGANIZATION(S) BELOW, NOR ANY PERSON ACTING ON BEHALF OF ANY OF THEM:

(A) MAKES ANY WARRANTY OR REPRESENTATION WHATSOEVER, EXPRESS OR IMPLIED, (I) WITH RESPECT TO THE USE OF ANY INFORMATION, APPARATUS, METHOD, PROCESS, OR SIMILAR ITEM DISCLOSED IN THIS DOCUMENT, INCLUDING MERCHANTABILITY AND FITNESS FOR A PARTICULAR PURPOSE, OR (II) THAT SUCH USE DOES NOT INFRINGE ON OR INTERFERE WITH PRIVATELY OWNED RIGHTS, INCLUDING ANY PARTY'S INTELLECTUAL PROPERTY, OR (III) THAT THIS DOCUMENT IS SUITABLE TO ANY PARTICULAR USER'S CIRCUMSTANCE; OR

(B) ASSUMES RESPONSIBILITY FOR ANY DAMAGES OR OTHER LIABILITY WHATSOEVER (INCLUDING ANY CONSEQUENTIAL DAMAGES, EVEN IF EPRI OR ANY EPRI REPRESENTATIVE HAS BEEN ADVISED OF THE POSSIBILITY OF SUCH DAMAGES) RESULTING FROM YOUR SELECTION OR USE OF THIS DOCUMENT OR ANY INFORMATION, APPARATUS, METHOD, PROCESS, OR SIMILAR ITEM DISCLOSED IN THIS DOCUMENT.

ORGANIZATION(S) THAT PREPARED THIS DOCUMENT

Iberdrola Ingenieria y Construccion SAU

NOTE

For further information about EPRI, call the EPRI Customer Assistance Center at 800.313.3774 or e-mail askepri@epri.com.

Electric Power Research Institute, EPRI, and TOGETHER SHAPING THE FUTURE OF ELECTRICITY are registered service marks of the Electric Power Research Institute, Inc.

Copyright © 2007 Electric Power Research Institute, Inc. All rights reserved.

CITATIONS

This report was prepared by

Iberdrola Ingenieria y Construccion SAU
Avenida de Burgos 8-B
Madrid. Spain 28036

Principal Investigator
Pablo J. Garcia
Andres Gomez
Consolacion Montalvo
Alberto Ortego

This report describes research sponsored by the Electric Power Research Institute (EPRI).

The report is a corporate document that should be cited in the literature in the following manner:

RETRAN-3D Analysis of BWR Control Rod Drop Accidents. EPRI, Palo Alto, CA: 2007.
1015206.

PRODUCT DESCRIPTION

The U.S. Nuclear Regulatory Commission (NRC) is currently revising the acceptance criteria applicable to boiling water reactor (BWR) control rod drop accidents (CRDA). To date, the NRC has proposed conservative rod failure and coolability limit criteria in Research Information Letter (RIL)-0401 and more recently as Interim Criteria in Revision 3 to Standard Review Plan (SRP) 4.2. EPRI is planning to develop reactivity initiated accident failure criteria appropriate to BWR CRDA under cold zero-power as well as hot zero-power conditions in order to propose a less restrictive set of criteria to the NRC. To achieve this objective, it is necessary to estimate the deposited energy and transient power histories that low-, intermediate-, and high-burnup fuel rods would experience during such accidents. CRDA analyses using RETRAN-3D kinetic methods have been performed in order to obtain these power histories.

Results & Findings

Different power evolutions have been found for cold zero-power (CZP) and hot zero-power (HZP) conditions. For CZP cases in which the startup conditions involve a large amount of initial subcooling, a significant portion of the total enthalpy is deposited following the initial prompt peak, thus forming a delayed power tail. The importance of the delayed power tail decreases with the amount of subcooling. For HZP conditions, effectively all the power is deposited in the first few milliseconds of the accident. This different behavior may have a significant impact on the failure mechanisms of the cladding resulting from pellet-cladding mechanical interaction (PCMI). These findings will be used by EPRI in a separate project in which the thermal-mechanical response of fuel subjected to such conditions will be determined in order to develop BWR failure thresholds and coolability limits.

Challenges & Objective(s)

- To perform detailed 3D kinetic analyses of BWR CRDA at different initial conditions.
- To evaluate the results obtained and determine their significance with respect to cladding failure criteria.

Applications, Values & Use

Application of this work should result in less restrictive cladding failure criteria than the proposed NRC Interim Criteria in Revision 3 to SRP 4.2 or in RIL-0401.

EPRI Perspective

The current work is part of an industrywide effort under EPRI's Fuel Reliability Program, aimed at ensuring safe and efficient operation of current plants, and possibly extending fuel rod average burnup levels above current licensing limits. The work was performed under the direction of Working Group 2 (Response to Transients) of the Fuel Reliability Program.

Approach

The project team performed detailed 3D kinetic analyses using the RETRAN-3D code for representative BWR conditions expected during CRDA. The team used best-estimate codes and model assumptions and analyzed both modern fuel design and high-burnup conditions. The analyses covered the range of operating temperatures expected during plant startup.

Keywords

Reactivity Initiated Accident (RIA)
Control Rod Drop Accidents (CRDA)
BWR Fuel
Fuel Reliability
Safety Analysis
RETRAN-3D Analysis

ABSTRACT

Within the Fuel Reliability Program, EPRI is planning to develop RIA failure criteria appropriate to BWR CRDA under cold zero-power (CZP) as well as hot zero-power (HZP) conditions. To achieve this objective, it is necessary to know the deposited energy and transient power histories that low, intermediate and high-burnup fuel rods would experience during such accidents.

Under this project Iberdrola Ingenieria y Construccion SAU (IBERINCO) has calculated power histories required for the development of RIA failure criteria by conducting a series of RETRAN CRDA calculations for a large BWR under CZP and HZP conditions.

The results of the RETRAN analyses provide a mapping of both the peak prompt enthalpy (enthalpy at the time of one pulse width after the peak power, *Full Width Half Max*) and the peak radially averaged maximum fuel enthalpy for the most energetic RIA rod drop accident as a function of bundle and nodal average exposure for different initial coolant temperature states that are possible during reactor startup. For cases in which the startup conditions involve a large amount of initial subcooling, a significant portion of the total enthalpy is found to be deposited after the initial prompt peak, thus forming a delayed power tail.

These findings will be used by EPRI in a separate project in which the thermal-mechanical response of fuel subjected to such conditions will be determined in order to develop failure thresholds and coolability limits appropriate for BWRs.

CONTENTS

1 INTRODUCTION	1-1
1.1 Background	1-1
1.2 Scope of Analysis.....	1-2
2 PLANT AND CORE DESCRIPTION	2-1
3 RETRAN-3D METHODOLOGY.....	3-1
3.1 Methodology Description.....	3-1
3.2 Methodology Validation.....	3-2
4 BWR CRDA STATIC ANALYSIS.....	4-1
4.1 Criticality Search	4-1
4.2 Worst Rod Search.....	4-6
5 BWR CRDA DYNAMIC ANALYSIS.....	5-1
5.1 RETRAN-3D Model.....	5-1
5.2 CRDA Static Comparisons	5-7
5.3 Power Results	5-10
5.4 Enthalpy Results	5-13
5.5 PCMI Failure Considerations	5-20
5.6 DNB Failure Considerations.....	5-23
6 CONCLUSIONS	6-1
7 REFERENCES	7-1

LIST OF FIGURES

Figure 1-1 Definition of Prompt Enthalpy Time (te).....	1-3
Figure 2-1 SVEA96-Optima-2 Average Enrichments in the Different Axial Segments	2-2
Figure 2-2 Equilibrium Cycle BOC Bundle Average Burnup (GWd/MT)	2-3
Figure 3-1 SIMTAB Methodology Diagram	3-1
Figure 3-2 Power Evolution Comparison for SPERT 81 Test	3-3
Figure 3-3 Power Evolution Comparison for SPERT 86 Test	3-3
Figure 3-4 Power Evolution Comparison for RAMONA T1 case (1.5\$)	3-4
Figure 3-5 Power Evolution Comparison for RAMONA T2 Case (2 \$)	3-4
Figure 3-6 Rod Worth Comparison SIMULATE-RETRAN	3-5
Figure 4-1 Critical Control Rod Configuration at 20°C	4-2
Figure 4-2 Critical Control Rod Configuration at 80°C	4-3
Figure 4-3 Critical Control Rod Configuration at 160°C	4-4
Figure 4-4 Critical Control Rod Configuration at 240°C	4-5
Figure 4-5 Bundle Burnup Distributions at EOC	4-7
Figure 5-1 CRDA RETRAN Axial Model	5-2
Figure 5-2 CRDA RETRAN Axial Model	5-3
Figure 5-3 Core Kinetic Nodalization	5-4
Figure 5-4 Initial Rod Map.....	5-5
Figure 5-5 Startup Pressure-Temperature Curves	5-6
Figure 5-6 Axial Power Comparison for 20°C Case.....	5-8
Figure 5-7 Axial Power Comparison for 80°C Case.....	5-9
Figure 5-8 Axial Power Comparison for 160°C Case.....	5-9
Figure 5-9 Axial Power Comparison for 240°C Case.....	5-10
Figure 5-10 Core Power Evolution for the 20°C Case	5-11
Figure 5-11 Core Power Evolution for the 80°C Case	5-11
Figure 5-12 Core Power Evolution for the 160°C Case	5-12
Figure 5-13 Core Power Evolution for 240°C Case	5-12
Figure 5-14 Detailed Peak Power Curves.....	5-13
Figure 5-15 Bundle Exposures (GWd/MT) Around the Dropped Rod.....	5-14
Figure 5-16 Enthalpy vs. Time for the 20°C Case.....	5-14
Figure 5-17 Enthalpy Rise vs. Burnup for the 20°C Case.....	5-15
Figure 5-18 Enthalpy Rise (cal/g) for Each Bundle in the 20°C Case.....	5-15

Figure 5-19 Enthalpy vs. Time for the 80°C Case.....	5-16
Figure 5-20 Enthalpy Rise vs. Burnup for the 80°C Case.....	5-16
Figure 5-21 Enthalpy Rise (cal/g) for Each Bundle in the 80°C Case.....	5-17
Figure 5-22 Enthalpy vs. Time for the 160°C Case.....	5-17
Figure 5-23 Enthalpy Rise vs. Burnup for the 160°C Case.....	5-18
Figure 5-24 Enthalpy Rise (cal/g) for Each Bundle in the 160°C Case.....	5-18
Figure 5-25 Enthalpy vs. Time for the 240°C Case.....	5-19
Figure 5-26 Enthalpy Rise vs. Burnup for the 240°C Case.....	5-19
Figure 5-27 Enthalpy Rise (cal/g) for Each Bundle in the 240°C Case.....	5-20
Figure 5-28 Ratio of Enthalpies as Function of Subcooling.....	5-21
Figure 5-29 Enthalpy Ratio vs. Bundle Burnup.....	5-22
Figure 5-30 Enthalpy Ratio vs. Maximum Enthalpy Rise.....	5-22
Figure 5-31 Prompt and Total Enthalpy vs. Initial Subcooling.....	5-23
Figure 5-32 Evolution of Cladding Temperature vs. Enthalpy Rise for the limiting Bundle in the 20°C Case.....	5-24
Figure 5-33 Cladding PCT vs. Total Enthalpy Rise for the Different Initial Temperatures.....	5-24
Figure 5-34 RETRAN DNB Prediction and Comparison with Experiments.....	5-25

LIST OF TABLES

Table 5-1 Static Variables Comparison for 20°C Case	5-7
Table 5-2 Static Variables Comparison for 80°C Case	5-7
Table 5-3 Static Variables Comparison for 160°C	5-7
Table 5-4 Static Variables Comparison for 240°C Case	5-7
Table 5-5 Rod Worth Comparisons	5-8
Table 5-6 Enthalpy Ratio as Function of Initial Subcooling.....	5-20

1

INTRODUCTION

1.1 Background

The licensing of light water reactors requires analysis of a set of design basis transients and accidents. One class of these accidents is the reactivity insertion accident (RIA), where the issues are the ability of the nuclear fuel to maintain its integrity in a fast power excursion, and the ability of the reactor coolant system to accommodate any resulting pressurization transient. The main concern is that in a fast power excursion enough energy could be deposited in the fuel rod in a very short period of time to cause cladding failure that results in loss of coolable geometry.

In a boiling water reactor (BWR), the most severe of this class of accidents is considered to be the control rod drop accident (CRDA). This accident is initiated by the decoupling of a control rod from its driving mechanism during a rod withdrawal maneuver, and the consequent sudden drop of the rod. The resulting insertion of positive reactivity into the core region around the dropped rod can cause the deposition of a large amount of energy in the fuel within a few hundred milliseconds.

If the core becomes supercritical during the rod drop, the core response will be characterized by a power excursion. This power excursion is initially stopped by the Doppler effect. The moderator temperature increase and void formation provide additional negative feedback after a few seconds. When the reactor trip setpoint is reached, the control rods are inserted into the core, and the power and temperature decrease back to the initial levels.

Acceptance criteria for CRDA events are based on GDC-28 requirements as it relates to the effects of postulated reactivity accidents neither resulting in damage to the reactor coolant pressure boundary greater than limited local yielding, nor causing sufficient damage to impair significantly the capacity to cool the core [1]. The specific acceptance criteria used currently for evaluating postulated CRDA events are:

1. Reactivity excursions should not result in a radially averaged enthalpy greater than 280 cal/g at any axial location in any fuel rod.
2. The maximum reactor pressure during any portion of the assumed excursion should be less than the value that will cause stresses to exceed the “Service Limit C” as defined in the ASME Boiler and Pressure Vessel Code, Section III, “Nuclear Power Plant Components”.
3. The number of fuel rods predicted to reach assumed fuel failure thresholds and associated parameters such as the amount of fuel reaching melting conditions will be an input to a radiological evaluation. The assumed failure thresholds are a radially averaged fuel rod enthalpy greater than 170 cal/g at any axial location for zero or low power initial conditions, and fuel cladding dryout for rated power initial conditions.

These acceptance criteria are under revision by the USNRC, and more restrictive criteria have been proposed based on USNRC's evaluation of RIA experiments performed on France and Japan with high burnup fuel rods, as reported in the RIL-0401 document [2]. Since the experimental results do not represent the conditions (initial temperatures, pulse widths...) expected in a BWR CRDA, a scaling technique was applied by the USNRC in order to generate the criteria proposed for application to real plant CRDAs.

Within the Fuel Reliability Program, EPRI is planning to develop RIA failure thresholds appropriate to BWR CRDA under cold zero-power (CZP) as well as hot zero-power (HZP) conditions. To achieve this objective, it is necessary to know the deposited energy and transient power histories that low, intermediate and high-burnup fuel rods would experience during such accidents.

1.2 Scope of Analysis

Under this project Iberdrola Ingenieria y Construcción SAU (IBERINCO) has calculated power histories required for the development of RIA failure criteria, by conducting a series of RETRAN CRDA calculations for a large BWR under CZP and HZP conditions.

The results of the RETRAN analyses provide a mapping of both the peak prompt enthalpy and the peak radially averaged maximum fuel enthalpy for the most energetic RIA rod drop accident as a function of bundle and nodal average exposure for different initial coolant temperature states that are possible during reactor startup. The prompt enthalpy is defined as the enthalpy at the time corresponding to one pulse width (Full Width Half Max) after the time of peak power. This time is more clearly defined in Figure 1-1. From that characterization, EPRI has selected specific result cases for use in a separate project for analysis of the fuel rod thermal-mechanical consequences and determination of the failure threshold and coolability limit.

Specific results or outputs from the RETRAN analysis include:

- Core power as a function of time
- Local power and axial power shape as a function of time
- Radial average peak fuel enthalpy as a function of time
- Local coolant temperature as a function of time and axial position
- Coolant pressure as a function of time
- Coolant flow velocity as a function of time and axial position
- Local cladding-coolant heat transfer coefficient as a function of time and axial position

In order to define the fuel rod failure threshold and coolability limit for modern BWR fuel, the neutron kinetics and thermal hydraulic calculations performed with RETRAN include modern 10x10 BWR fuel designs at extended burnup conditions under the most aggressive RIA conditions.

The following conditions have been represented:

1. Fuel design: Calculations have been performed for a 24 months equilibrium cycle operating at power uprate conditions. The fuel type selected is a modern 10x10 type with a bundle average enrichment of 4.20%. This design is the highest bundle enrichment presently available within the limitation of 4.95% maximum pellet enrichment.
2. Burnup: The CRDA calculations have been performed at end of cycle (EOC) conditions. This implies obtaining the highest burnup as possible in the bundles around the limiting dropped rod. Bundle average burnups of around 55 GWd/MT have been searched as objective. This will imply a peak pellet burnup of around 70 GWd/MT.
3. Coolant temperature: RETRAN calculations have been performed at 20, 80, 160 and 240°C. The critical conditions during startup corresponding to each temperature have been searched, and then the limiting dropped rod.
4. Coolant pressure: Minimum allowable coolant pressures for coolant temperature conditions for CZP and HZP will be used conservatively in the mechanical calculations. For the core kinetic calculations the maximum allowable coolant pressures for the coolant temperatures have been conservatively used. This delays the void formation during the RIA and maximizes the fuel average enthalpy obtained during the accident.
5. Searching of the highest worth rod to give the maximum pulse height and narrowest pulse width: In order to have significant enthalpy values the analyses have assumed that the Bank Position Withdrawal Sequence system (BPWS) restrictions are bypassed. The search of rods has been focused on the following limits:
 - a. A rod worth of at least 3.0\$. (This value is well above the rod worths expected in specific plant applications within the BPWS restrictions).
 - b. A maximum enthalpy rise calculated in the limiting bundle of at least 170 cal/g.

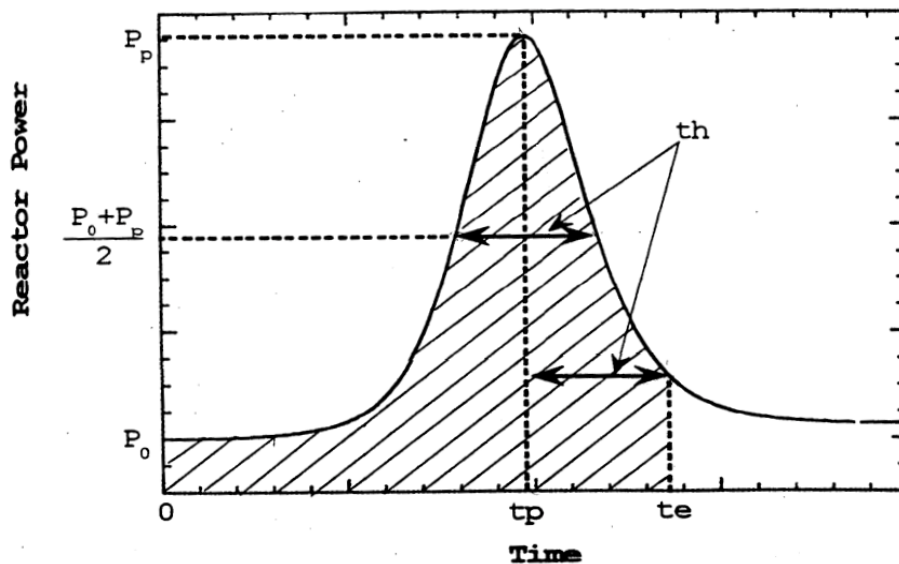


Figure 1-1
Definition of Prompt Enthalpy Time (t_e)

2

PLANT AND CORE DESCRIPTION

The analyses have been performed for Cofrentes NPP. Cofrentes is a GE BWR-6 design with 624 fuel bundles, in operation since 1984, owned and operated by Iberdrola and located in Valencia (Spain). The plant is operating at an extended power uprate of 3237 MWt (111.85% of the initial power) and is presently in cycle 16, a 22 months length cycle in transition to a 24 month cycle expected for cycle 17.

The plant is operating with a mixed core conformed by fuel bundles from GNF (GE-12 and GE-14), Westinghouse (SVEA-96 and SVEA-96-OPTIMA-2) and F-ANP (Atrium-10XP). For the CRDA analyses an equilibrium cycle composed of SVEA-96 OPTIMA 2 fuel and with a cycle length of 24 months has been selected.

The core for that equilibrium cycle is composed of 292 bundles of OPT42015GZ and 332 bundles of OPT42114GZ designs in a conventional loading pattern. A total of 256 fresh bundles are loaded (41% loading fraction): 136 of OPT42015GZ design and 120 of OPT42114GZ design.

Figure 2-1 describes the design of the bundles. Figure 2-2 describes the beginning of cycle (BOC) bundle average burnup corresponding to the conventional loading pattern.

The 24 month cycle exposure has been extended up to 25.4 GWd/MT, including operation with Final Feedwater Temperature Reduction (FFWTR) and power coastdown and considering the uncertainties in the target Keff. This burnup extension has been applied in order to obtain the highest as possible bundle burnups at end of cycle (EOC), where the CRDA calculations are to be performed.

OPT- 420-15GZ	OPT- 421-14GZ
Segment:8 OPT 071 NOGV 15.24 cm	Segment: 13 OPT 071 NOGV 15.24 cm
Segment :7 OPT 450 4G5 9G9V 106.68 cm	Segment: 12 OPT 452 5G5 9G9V 106.68 cm
Segment: 6 OPT 453 6G5 9G9V 137.16 cm	Segment: 11 OPT 455 5G5 9G9V 137.16 cm
Segment: 5 OPT 446 6G5 9G9 106.68 cm	Segment: 10 OPT 448 5G5 9G9 106.68 cm
Segment: 4 OPT 071 NOG 15.24 cm	Segment: 9 OPT 071 NOG 15.24 cm

Figure 2-1
SVEA96-Optima-2 Average Enrichments in the Different Axial Segments

EXP	2D	MAP	(GWd/Tm)				0,9072																													
	2	14	1	1	28	0	1																													
	1	3	5	7	9	11	13	15	17	19	21	23	25	27	29	31	33	35	37	39	41	43	45	47	49	51	53	55								
56											47,27	44,73	44,30	40,61	40,55	44,28	45,04	47,54																		
54								48,61	42,68	38,46	37,75	22,58	22,20	24,55	24,34	22,00	22,78	37,81	38,11	42,71	48,55															
52							47,59	38,24	22,38	20,53	0,00	0,00	0,00	0,00	0,00	0,00	0,00	0,00	0,00	20,32	22,20	38,19	47,56													
50						47,28	37,33	21,91	0,00	0,00	22,85	0,00	24,99	0,00	0,00	24,77	0,00	23,06	0,00	0,00	21,69	37,31	47,62													
48					41,12	36,90	0,00	0,00	20,73	25,76	0,00	25,76	0,00	26,58	26,74	0,00	25,90	0,00	25,57	20,92	0,00	0,00	36,90	41,13												
46				48,02	36,86	19,18	0,00	0,00	24,88	0,00	25,69	0,00	26,01	0,00	0,00	25,81	0,00	25,82	0,00	25,09	0,00	0,00	19,00	36,94	47,82											
44			47,00	37,66	0,00	0,00	18,79	26,03	0,00	25,98	0,00	26,05	0,00	26,49	26,65	0,00	26,23	0,00	25,74	0,00	26,18	19,02	0,00	0,00	37,34	47,274										
42		48,31	38,08	21,96	0,00	0,00	25,53	0,00	25,33	0,00	26,40	0,00	25,83	0,00	0,00	26,03	0,00	26,21	0,00	25,49	0,00	25,31	0,00	0,00	21,71	38,229	48,620									
40		42,37	22,00	0,00	21,11	25,37	0,00	25,36	0,00	26,61	0,00	25,82	0,00	26,71	26,52	0,00	25,96	0,00	26,79	0,00	25,54	0,00	25,13	20,95	0,00	22,232	42,637									
38		38,48	20,57	0,00	25,03	0,00	25,97	0,00	26,98	0,00	26,28	0,00	26,16	0,00	0,00	26,33	0,00	26,48	0,00	26,78	0,00	25,74	0,00	25,21	0,00	20,337	38,142									
36	47,68	38,01	0,00	23,33	0,00	25,71	0,00	26,05	0,00	26,67	0,00	26,50	0,00	25,33	25,54	0,00	26,31	0,00	26,48	0,00	26,26	0,00	25,88	0,00	23,08	0,00	37,835	47,662								
34	45,11	22,99	0,00	0,00	25,69	0,00	26,50	0,00	25,82	0,00	26,12	0,00	26,54	0,00	0,00	26,31	0,00	26,32	0,00	25,98	0,00	26,34	0,00	25,47	0,00	0,00	22,815	45,093								
32	44,70	21,81	0,00	25,04	0,00	25,67	0,00	26,34	0,00	26,53	0,00	26,54	0,00	22,57	22,78	0,00	26,32	0,00	26,36	0,00	26,20	0,00	25,85	0,00	24,80	0,00	22,050	44,318								
30	40,51	24,22	0,00	0,00	26,65	0,00	26,55	0,00	26,34	0,00	25,84	0,00	23,03	36,87	36,86	22,79	0,00	25,71	0,00	26,52	0,00	26,66	0,00	26,76	0,00	0,00	24,463	40,650								
28	40,59	24,47	0,00	0,00	26,44	0,00	26,34	0,00	26,56	0,00	25,67	0,00	22,86	36,54	36,52	22,58	0,00	25,50	0,00	26,70	0,00	26,50	0,00	26,60	0,00	0,00	24,654	40,688								
26	44,72	22,07	0,00	25,21	0,00	25,90	0,00	26,18	0,00	26,39	0,00	26,73	0,00	22,86	23,02	0,00	26,55	0,00	26,17	0,00	26,00	0,00	26,04	0,00	25,01	0,00	22,249	44,338								
24	44,79	22,85	0,00	0,00	25,86	0,00	26,36	0,00	25,63	0,00	26,35	0,00	26,72	0,00	0,00	26,53	0,00	26,51	0,00	25,84	0,00	26,16	0,00	25,70	0,00	0,00	22,622	44,784								
22	47,41	37,99	0,00	23,16	0,00	25,54	0,00	26,27	0,00	26,51	0,00	26,35	0,00	25,50	25,67	0,00	26,11	0,00	26,28	0,00	26,45	0,00	25,74	0,00	22,86	0,00	37,782	47,388								
20		38,76	20,73	0,00	24,81	0,00	26,16	0,00	26,83	0,00	26,51	0,00	26,37	0,00	0,00	26,51	0,00	26,67	0,00	26,59	0,00	25,98	0,00	25,04	0,00	20,549	38,49									
18		42,33	22,22	0,00	20,98	25,20	0,00	25,15	0,00	26,86	0,00	25,62	0,00	26,59	26,35	0,00	25,81	0,00	27,00	0,00	25,38	0,00	24,92	20,77	0,00	22,402	42,585									
16		48,38	38,16	22,13	0,00	0,00	25,71	0,00	25,11	0,00	26,23	0,00	26,01	0,00	0,00	26,18	0,00	26,01	0,00	25,32	0,00	25,52	0,00	0,00	21,92	38,275	48,675									
14			46,68	37,68	0,00	0,00	19,02	25,85	0,00	26,17	0,00	26,26	0,00	26,35	26,55	0,00	26,38	0,00	25,97	0,00	26,03	19,20	0,00	0,00	37,36	47,023										
12				47,75	36,93	18,99	0,00	0,00	25,17	0,00	25,48	0,00	25,87	0,00	0,00	25,63	0,00	25,65	0,00	25,34	0,00	0,00	18,76	36,93	47,48											
10					41,43	36,89	0,00	0,00	20,93	25,91	0,00	25,56	0,00	26,45	26,64	0,00	25,76	0,00	25,77	21,07	0,00	0,00	36,81	41,43												
8						47,56	37,65	22,13	0,00	0,00	23,16	0,00	25,21	0,00	0,00	25,02	0,00	23,33	0,00	0,00	21,96	37,63	47,84													
6							47,53	38,13	22,20	20,72	0,00	0,00	0,00	0,00	0,00	0,00	0,00	0,00	0,00	20,55	21,96	38,03	47,57													
4								48,32	42,44	38,72	37,96	22,80	22,01	24,36	24,10	21,76	22,95	37,98	38,44	42,45	48,24															
2											47,29	44,76	44,70	40,51	40,41	44,68	45,07	47,55																		

Figure 2-2
Equilibrium Cycle BOC Bundle Average Burnup (GWd/MT)

3

RETRAN-3D METHODOLOGY

3.1 Methodology Description

The code used in the 3D dynamic analysis is RETRAN-3D [3]. IBERINCO is using the 3D feature of RETRAN as standard method for the analysis of the BWR CRDA and other asymmetric accidents. The core design is performed with the CASMO/SIMULATE package. A set of 3D cross sections is generated from SIMULATE [4]. In order to do it a methodology (SIMTAB) has been developed [5]. This methodology collapses the kinetic information from SIMULATE and converts it to the format required by RETRAN.

Figure 3-1 summarizes the process used to generate the kinetic data. To verify the adequacy of the process before the RETRAN dynamic analysis is performed, the RETRAN -3D values of the relevant static variables are compared with the SIMULATE results.

The variables used and the typical acceptable differences are described in the Section 3.2

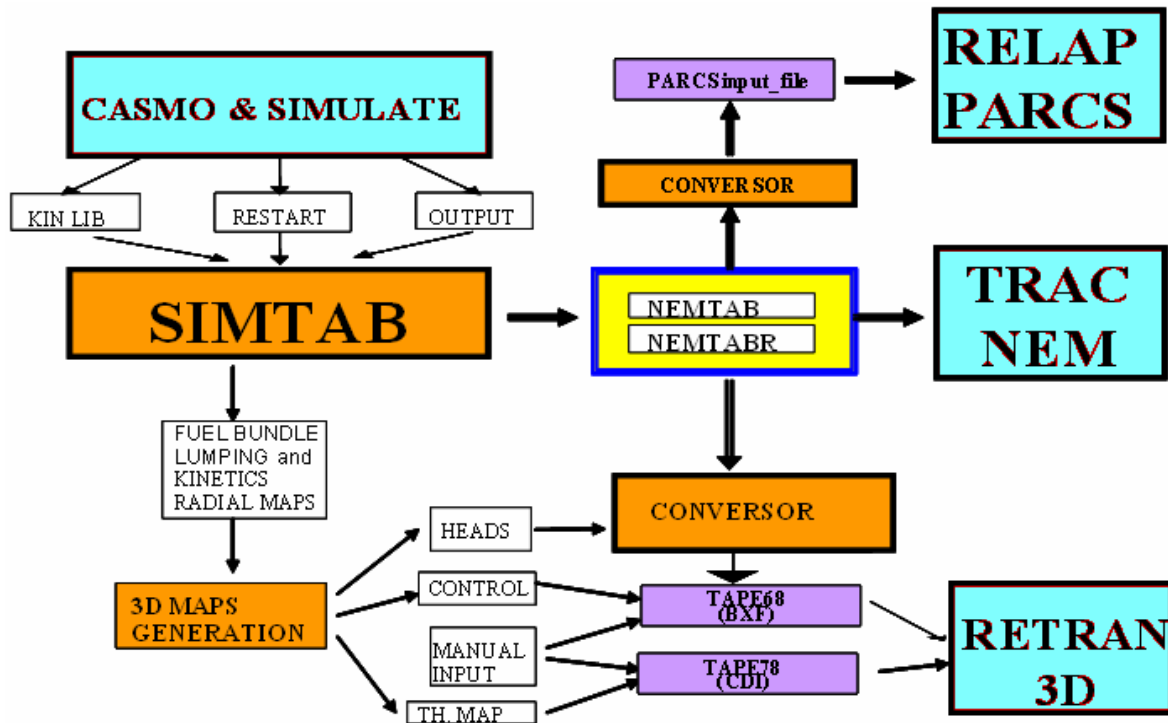


Figure 3-1
SIMTAB Methodology Diagram

3.2 Methodology Validation

The 3D kinetic model of RETRAN-3D has been accepted for licensing purposes by the US-NRC and has been used in several 3D kinetics benchmarks [6]. IBERINCO has additionally performed its own validation, consisting of:

- Reproduction of the SPERT 81 and 86 tests
- Comparison with Cofrentes licensing CRDA analysis performed with RAMONA-3 code by Westinghouse

The results obtained in these comparisons are shown in Figures 3-2 to 3-5. Additional information of these comparisons has been presented in the Water Reactor Fuel Performance Meeting held in Kyoto in October 2005 [7].

The process to generate the cross section package from SIMULATE is validated for every RETRAN-3D case before performing the dynamic analyses. To verify the adequacy of the process the following relevant RETRAN-3D variables are compared with the SIMULATE results:

- Initial Keff values
- Initial beta effective values
- Initial power distributions
- Dropped rod worth values

Typical differences obtained in these comparisons are: less than 1% DK in the Keff, less than 15% differences in the power peak values, axial offset and rod worth values and less than 5% in the beta effective. These values are in the order of the prediction accuracy of the neutronic code.

A typical comparison of rod worth values between SIMULATE and RETRAN for CZP and HZP conditions can be seen in Figure 3-6.

These differences are similar to those obtained in other methodologies where different codes are used for the static and dynamic RIA analysis and are covered by the conservatisms used in the licensing models [8],[9].

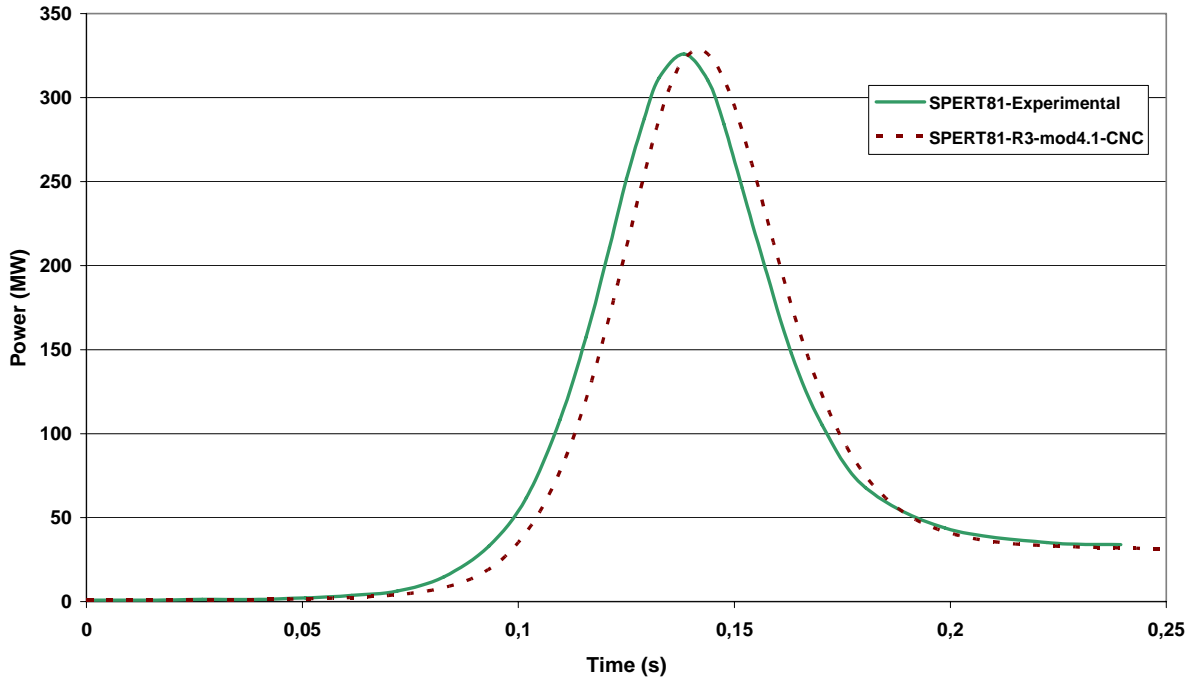


Figure 3-2
Power Evolution Comparison for SPERT 81 Test

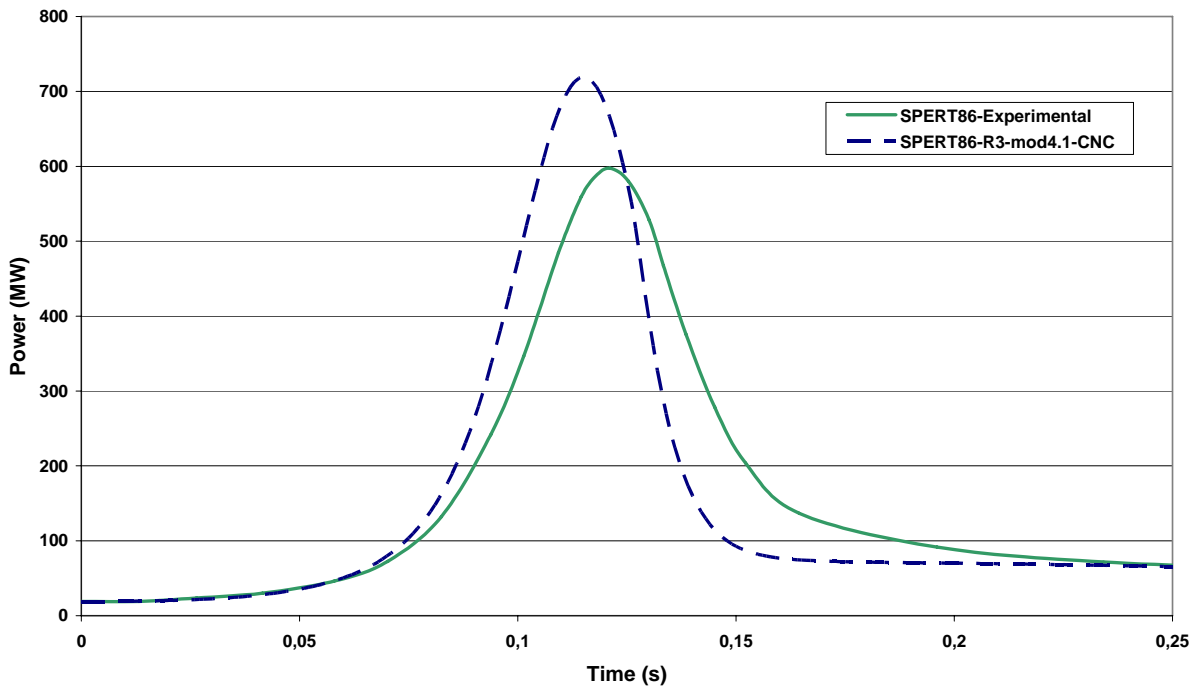


Figure 3-3
Power Evolution Comparison for SPERT 86 Test

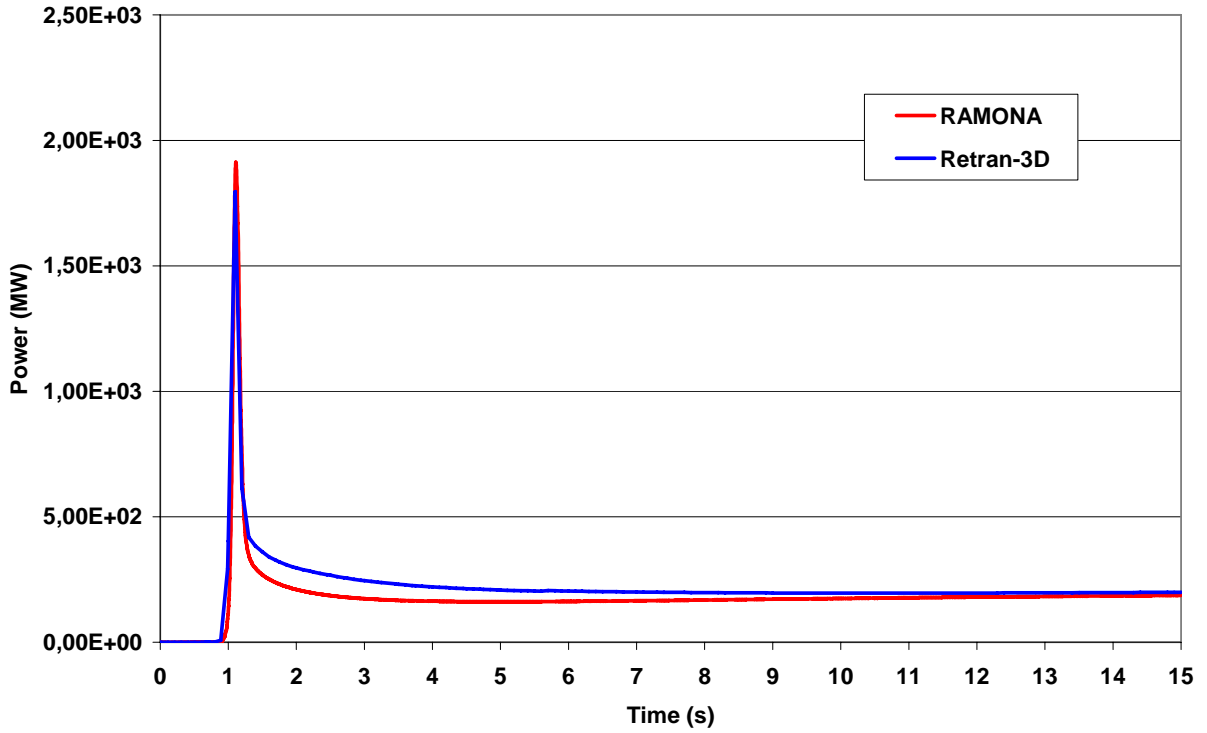


Figure 3-4
Power Evolution Comparison for RAMONA T1 case (1.5\$)

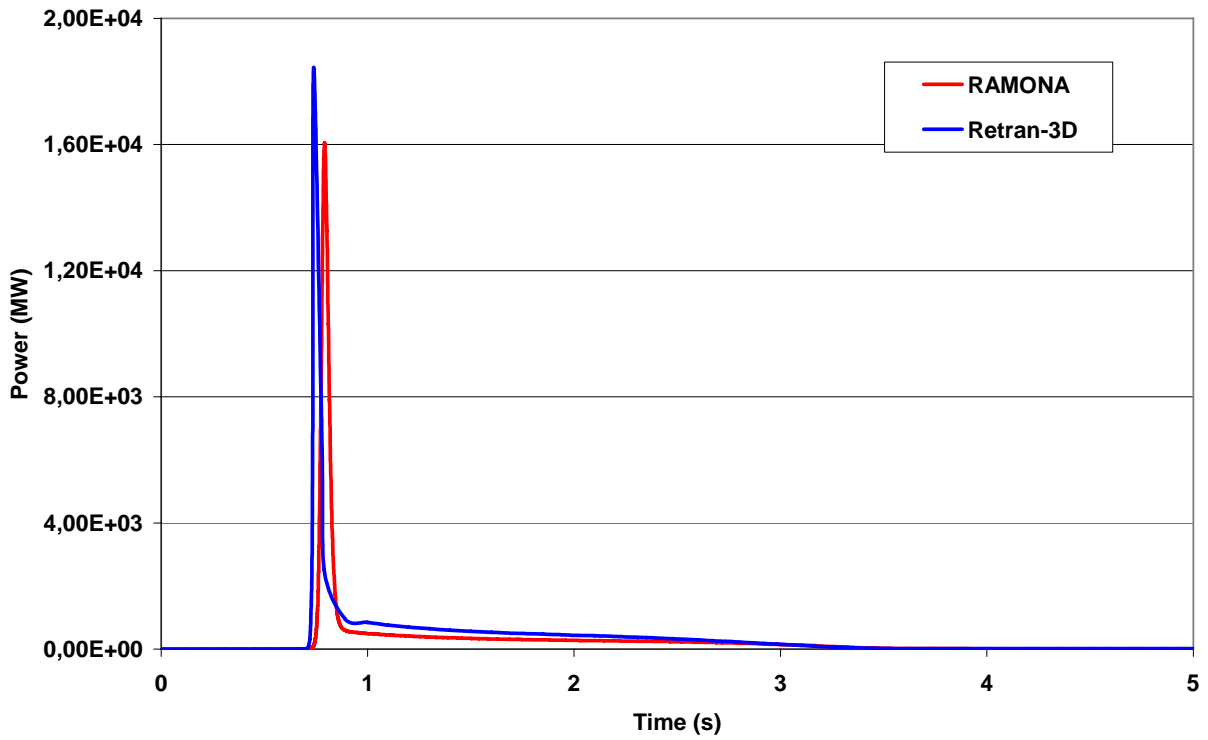


Figure 3-5
Power Evolution Comparison for RAMONA T2 Case (2 \$)

Comparison of rod worth values

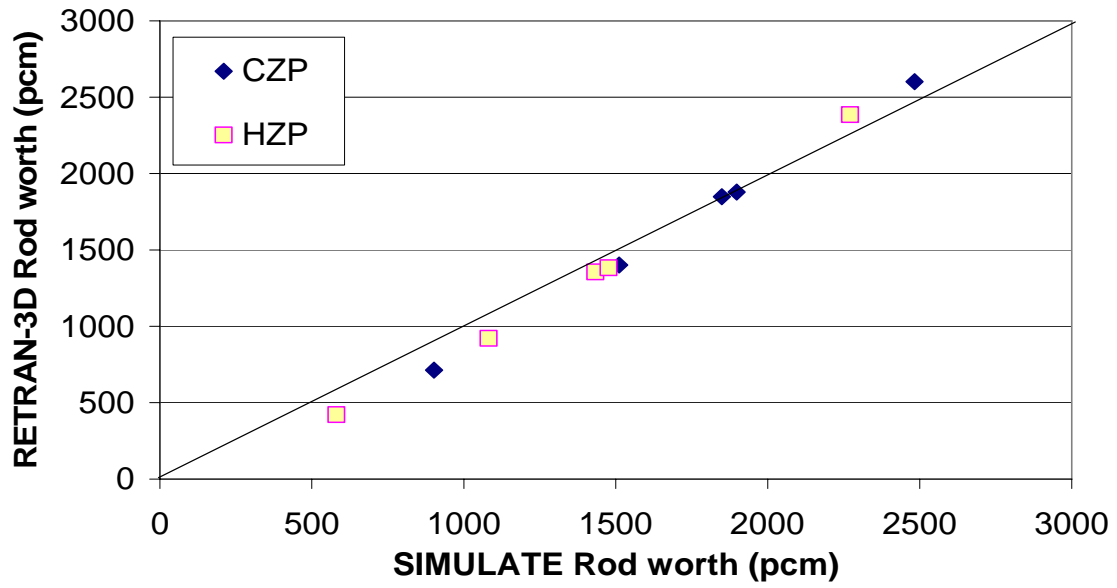


Figure 3-6
Rod Worth Comparison SIMULATE-RETRAN

4

BWR CRDA STATIC ANALYSIS

4.1 Criticality Search

As indicated in Section 2 of this report, the CRDA calculations are performed at the end of an equilibrium cycle in order to have the highest burnup as possible in the bundles surrounding the dropped rod.

At this EOC (including cycle extensions) point, critical conditions are searched following the startup procedures for each one of the temperatures of analysis. The dynamic CRDA analyses are to cover the range of the possible temperatures during startup conditions. The temperatures chosen are: 20°C, 80°C, 160°C and 240°C.

For each of these temperatures the control rod configuration at which the core reaches criticality within the uncertainties of the target K_{eff} is searched. SIMULATE-3 code is used for this. Figures 4-1 to 4-4 indicate the critical configuration found for each temperature. The rod positions in blank are fully inserted. The rods at 48 are fully withdrawn. As can be seen the critical conditions are found at relatively similar rod configurations and close to the 50% control rod density (groups 1 to 4 fully withdrawn, groups 5 to 10 fully inserted). The critical rod belongs in all the cases to group 4 with groups 1,2 and 3 withdrawn, and groups 5,7,8,9 and 10 inserted. This situation is due to the fact that the modern fuel designs have a positive moderator temperature coefficient at high burnup conditions. In this way the positive reactivity added by the moderator during the heatup compensates for the always negative reactivity added by the Doppler coefficient. This results in a similar configuration of control rods in critical conditions.

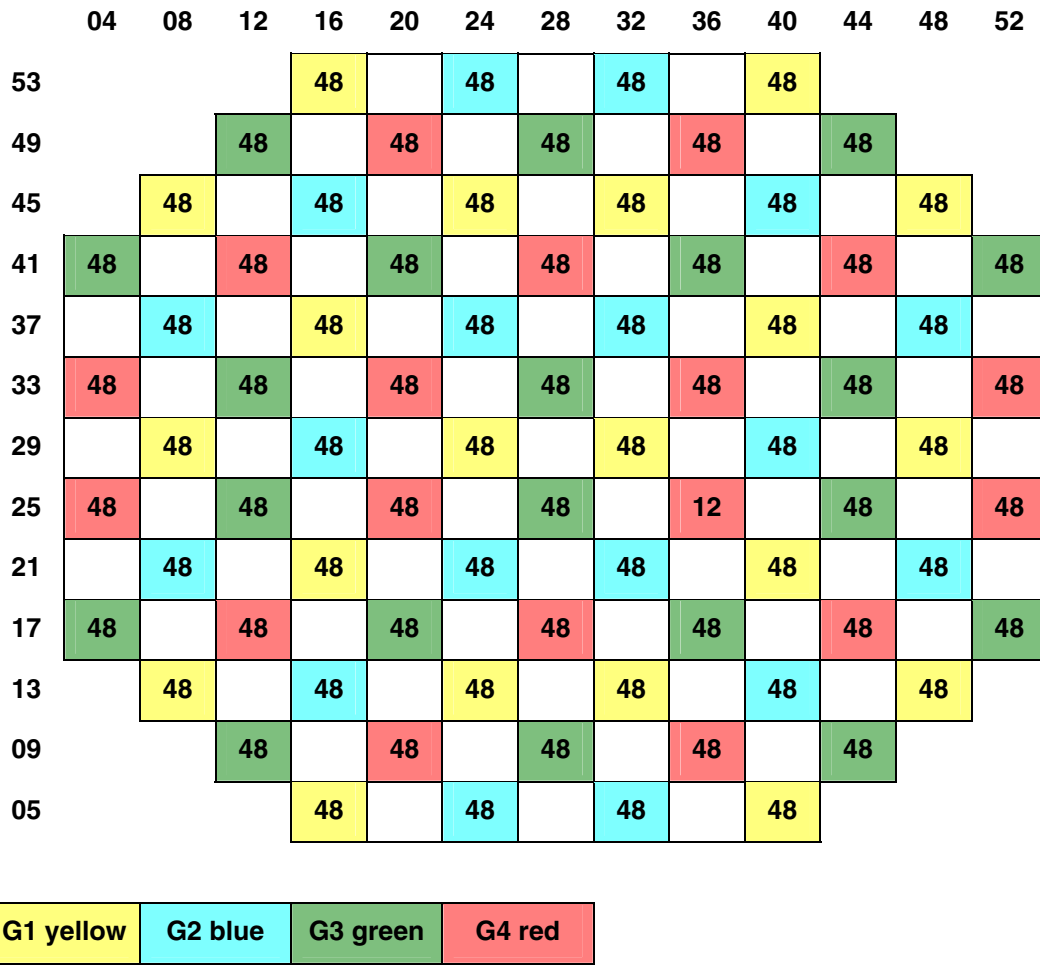


Figure 4-1
Critical Control Rod Configuration at 20°C

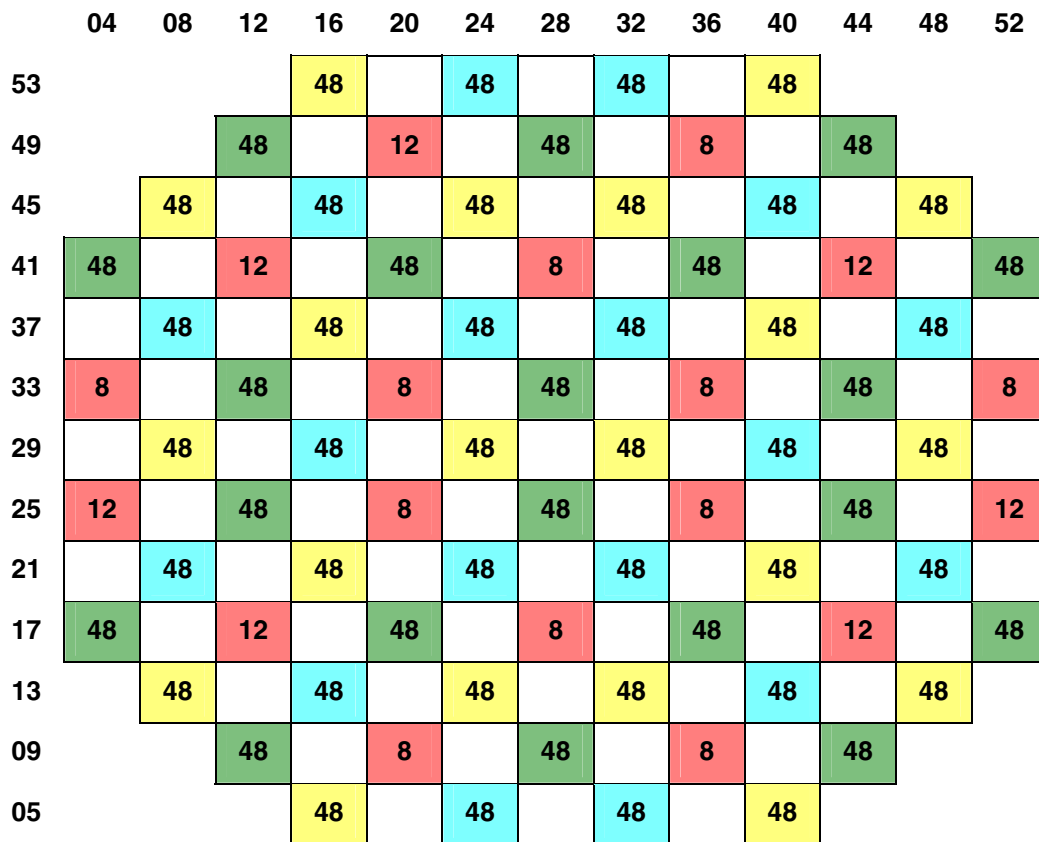


Figure 4-2
Critical Control Rod Configuration at 80°C

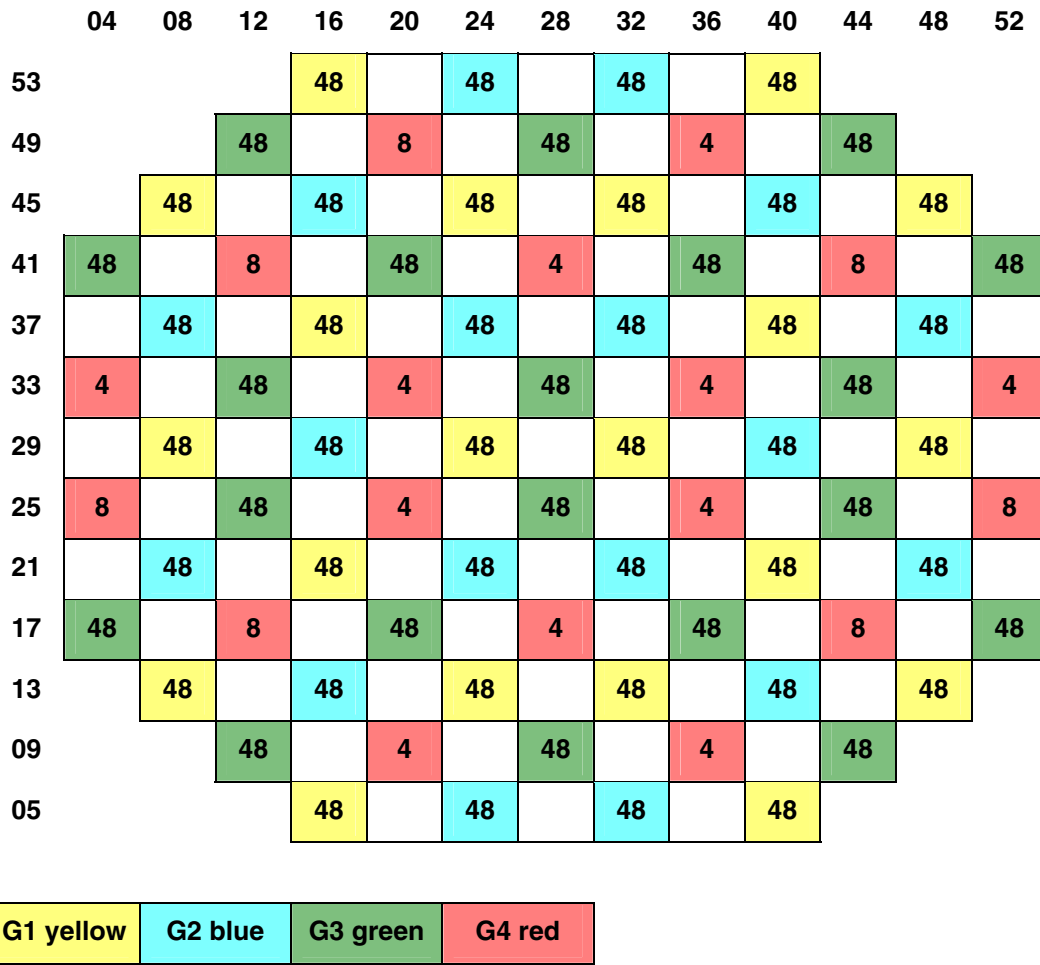


Figure 4-3
Critical Control Rod Configuration at 160°C

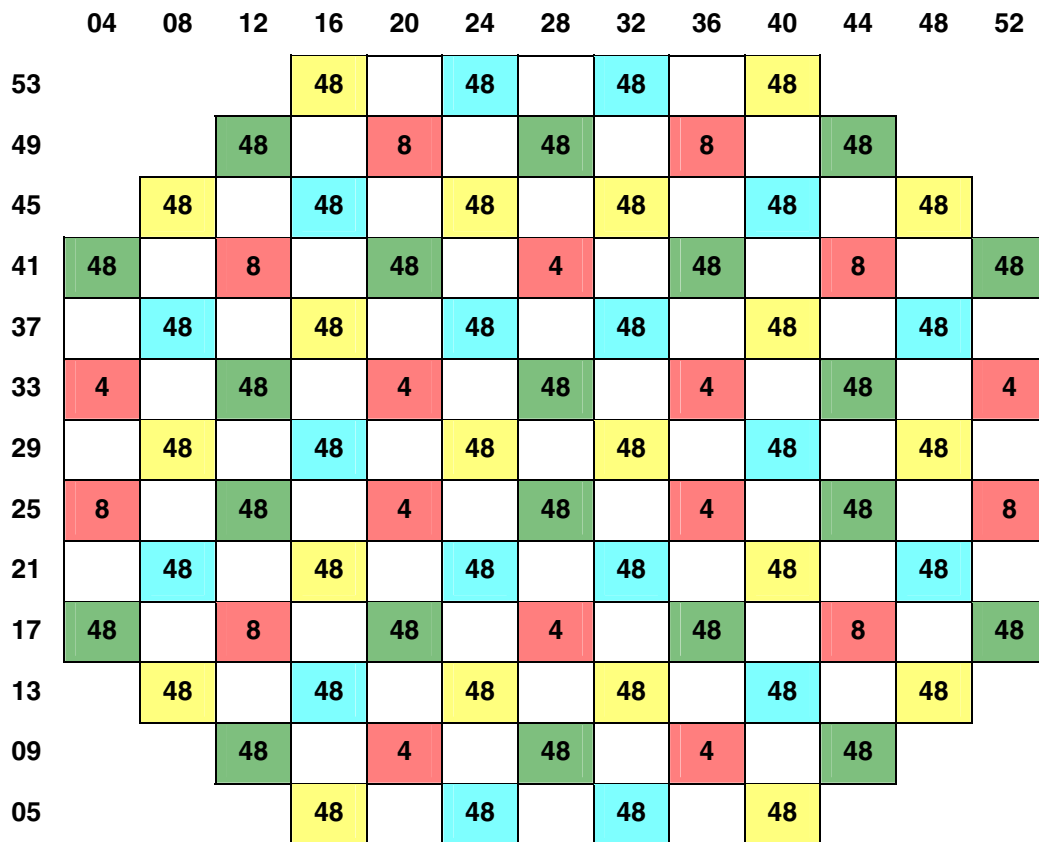


Figure 4-4
Critical Control Rod Configuration at 240°C

4.2 Worst Rod Search

Starting from each one of the critical conditions, a search for the highest worth rod is performed using the Iberdrola licensed control rod worth search methodology [10]. SIMULATE-3 code is used for this. This methodology has been used for each Cofrentes NPP reload licensing since 1998, to determine the highest rod worth expected during a CRDA and following the constraints of the Bank Position Withdrawal Sequence (BPWS) system. These rod worths are compared every reload with the fuel vendor generic enthalpy rise vs. rod worth curves to verify the CRDA acceptance criteria.

For each case the highest worth rods found were the rods in positions (28, 53) and (24, 49). Rod in position (28, 53) belongs to group 10 and rod in position (24, 49) belongs to group 7. Since rod (24, 49) is adjacent to a higher burnup bundle (54.2 GWd/MT), this rod is selected for the CRDA dynamic analysis. Figure 4-5 represents the burnup distributions at EOC as well as the control rod position.

In order to have the highest dropped rod worth as possible, the rod (24, 49) is assumed to be withdrawn as the first rod of its group (starting from a 50% control rod density configuration) and to drop from fully inserted to fully withdrawn position. These assumptions imply the bypassing of the Bank Position Withdrawal Sequence system (BPWS). This system determines the rod withdrawal sequence and is designed to minimize the rod worths during the plant startup and has to be bypassed in order to have significant enough rod worth values [11].

Assuming that the BPWS system is bypassed the worth obtained for the (24, 49) rod is around 3.5\$. If the rod (24, 49) is assumed to be the first rod withdrawn after the 50% rod density configuration, but to drop within the constraints of the BPWS system, the rod worth would be limited to 1.7\$

2D	MAP	(GWd/Tm)	0.907																																					
2	14	1	1	28	0	1																					29	31	33	35	37	39	41	43	45	47	49	51	53	55
	1	3	5	7	9	11	13	15	17	19	21	23	25	27	29	31	33	35	37	39	41	43	45	47	49	51	53	55												
56	0.000									55.122	53.821	54.442	51.262	51.213	54.437	54.074	55.348																							
54										55.401	52.154	50.592	52.436	41.610	42.273	44.654	44.633	42.255	41.629	52.392	50.320	52.195	55.363																	
52										56.075	50.940	40.575	41.458	25.543	27.198	27.995	28.359	28.629	28.261	26.925	25.285	41.495	40.619	50.809	56.036															
50										56.560	51.530	42.583	25.746	27.954	49.352	30.851	52.181	30.930	31.197	52.241	30.572	49.274	28.220	26.000	42.209	51.366	56.849													
48										51.108	51.613	23.980	27.566	47.426	52.634	32.060	54.250	32.785	54.703	54.983	32.985	54.170	31.835	52.660	47.718	27.329	23.768	51.680	51.144											
46										57.294	51.513	41.301	27.884	30.363	52.524	31.808	54.109	33.037	54.683	32.882	33.086	54.700	32.809	54.021	31.993	52.821	30.119	27.672	41.335	51.727	57.159									
44										55.528	51.738	23.505	27.402	46.410	53.620	32.158	54.124	32.878	54.799	32.982	54.996	55.326	33.223	54.683	32.600	54.148	32.393	53.491	46.366	27.707	23.805	51.412	55.788							
42										55.161	50.826	42.618	27.076	29.922	53.257	31.770	53.439	32.470	54.953	32.465	53.993	32.707	32.963	54.347	32.176	54.576	32.714	53.765	31.505	52.892	30.237	27.380	42.252	50.860	55.438					
40										51.900	40.619	26.224	47.719	52.922	32.686	53.858	32.433	54.895	32.942	54.258	32.299	55.082	55.098	32.486	54.166	32.714	55.183	32.630	53.823	32.507	52.944	47.793	26.031	40.660	52.127					
38										50.626	41.864	28.456	52.056	31.819	54.506	32.933	55.153	31.856	54.196	32.815	54.514	31.476	31.683	54.810	32.594	54.160	32.057	55.183	32.730	54.175	32.040	52.359	28.245	41.521	50.354					
36	55.467	52.564	25.568	49.729	31.616	53.737	32.859	54.680	32.446	54.076	31.754	54.694	32.083	52.582	52.963	32.351	54.331	31.490	54.151	32.711	54.611	32.600	54.082	31.863	49.304	25.297	52.418	55.456												
34	54.148	41.824	27.234	30.882	53.829	32.540	55.080	32.424	53.826	32.321	54.392	32.007	53.730	31.450	31.720	53.805	31.775	54.333	32.595	54.166	32.156	54.738	32.784	53.865	30.592	26.933	41.657	54.118												
32	54.816	42.152	28.535	52.669	32.828	54.421	33.406	54.655	32.261	54.759	32.650	54.135	31.091	50.051	50.382	31.328	53.839	32.477	54.814	32.471	54.373	33.180	54.705	32.995	52.278	28.266	42.292	54.464												
30	51.195	44.600	28.919	31.502	54.820	32.906	55.420	33.158	54.786	31.451	53.290	31.994	50.369	60.161	60.290	50.402	31.842	53.069	31.684	55.090	32.937	55.304	33.072	55.024	31.231	28.631	44.726	51.286												
28	51.270	44.649	28.706	31.289	54.449	32.644	55.103	32.955	54.739	31.184	52.993	31.779	50.021	59.732	59.895	50.071	31.572	52.693	31.478	55.063	32.680	54.970	32.864	54.730	30.960	28.359	44.732	51.323												
26	54.816	42.208	28.322	52.612	32.566	54.378	33.211	54.377	32.012	54.436	32.434	54.075	30.805	50.023	50.373	31.100	53.763	32.210	54.513	32.284	54.021	32.934	54.676	32.783	52.201	27.996	42.306	54.465												
24	53.889	41.846	27.439	31.095	54.180	32.810	55.169	32.651	53.923	32.589	54.726	32.181	54.049	31.663	31.879	54.107	32.011	54.694	32.815	54.257	32.444	54.839	33.002	54.204	30.861	27.202	41.642	53.864												
22	55.237	52.642	25.768	49.792	31.897	53.855	33.083	55.031	32.723	54.183	31.951	54.728	32.308	52.892	53.194	32.526	54.392	31.754	54.185	32.937	54.987	32.876	54.170	32.086	49.382	25.554	52.467	55.224												
20	50.848	41.846	28.269	51.706	31.593	54.494	32.737	54.831	31.591	54.195	32.590	54.436	31.183	31.448	54.754	32.321	54.087	31.854	54.889	32.479	54.147	31.860	52.086	27.994	41.489	50.629														
18	51.861	40.664	26.047	47.444	52.616	32.502	53.539	32.177	54.842	32.727	53.926	32.026	54.770	54.806	32.275	53.827	32.449	55.155	32.426	53.485	32.261	52.643	47.517	25.790	40.616	52.069														
16	55.223	50.981	42.918	27.380	30.219	53.570	31.979	53.489	32.723	54.997	32.673	54.356	32.983	33.186	54.636	32.443	54.644	32.913	53.797	31.755	53.268	30.466	27.618	42.629	50.999	55.481														
14	55.268	51.884	23.778	27.669	46.741	53.624	32.395	54.469	33.084	55.131	33.263	55.139	55.453	33.453	55.028	32.857	54.474	32.567	53.562	46.700	27.909	24.019	51.583	55.584																
12	57.076	51.483	40.936	27.638	30.107	52.494	31.529	53.789	32.855	54.399	32.669	32.928	54.429	32.574	53.671	31.759	52.798	29.793	27.360	40.974	51.661	56.879																		
10	51.360	51.427	23.736	27.316	47.327	52.511	31.869	53.969	32.583	54.446	54.803	32.833	53.875	31.587	52.612	47.617	27.013	23.465	51.458	51.389																				
8	56.764	51.821	42.868	25.984	28.215	49.771	31.097	52.616	31.265	31.477	52.654	30.873	49.706	28.414	26.173	42.571	51.683	56.990																						
6	56.005	50.912	40.608	41.812	25.756	27.442	28.329	28.713	28.924	28.537	27.232	25.557	41.832	40.564	50.763	56.025																								
4	55.134	51.950	50.806	52.609	41.810	42.173	44.572	44.506	42.114	41.791	52.534	50.588	51.973	55.076																										
2	55.138	53.866	54.807	51.214	51.124	54.802	54.125	55.360																																

Figure 4-5
Bundle Burnup Distributions at EOC

5

BWR CRDA DYNAMIC ANALYSIS

5.1 RETRAN-3D Model

The CRDA dynamic analyses are performed with the RETRAN-3D code. The 3D core kinetic module of RETRAN is used. Since the CRDA is a core kinetic accident the modelization is limited to the core. A detailed 3D core model with boundary conditions is sufficient to characterize the simulation, as represented in Figure 5-1.

The core model is formed by a cubic matrix of 28x28x25 active cells surrounded by the reflectors, plus the bypass composed by 25 volumes. Both core and bypass are linked in the bottom by the lower plenum and in the top by the upper plenum.

The 3D model is characterized by a thermohydraulic nodalization and a kinetic nodalization. The thermohydraulic nodalization consists of 54 channels; see Figure 5-2, with a more detailed nodalization around the dropped rod. Since the dropped rod is asymmetric, an asymmetric model is used. The initial radial power distribution is also considered to define the nodalization criteria. Each hydraulic channel is divided axially in 25 nodes. The same initial flow is assumed in each channel.

The kinetic model is formed by 4353 different fuel compositions. These compositions result in 175 different kinetic elements as indicated in Figure 5-3. The kinetic cross sections are obtained from SIMULATE through the SIMTAB method described in Section 3 of this report.

The initial control rod pattern and rod grouping is illustrated in Figure 5-4. There are three groups of rods in a checkerboard configuration typical of the 50% rod density. Group 3 represents the dropped rod. Group 1 represents the fully inserted rods and group 2 represents the withdrawn rods.

The core is composed of 624 bundles of SVEA-96-Optima 2 fuel. The RETRAN-3D analysis are performed using the following model approaches:

- Direct moderator heating: 2%
- Direct bypass heating: 2%
- Rod drop velocity: 1 m/s
- Scram signal: 134.6% of rated neutron flux
- Scram average speed: 1.316 m/s with a 0.19 s delay
- Credit to the moderator reactivity feedback due to void formation during the accident

- Startup initial conditions: Zero (30 W) power, 20% of nominal core flow

For each initial coolant temperature there is a range of possible vessel pressures. The range is represented in Figure 5-5. The minimum pressure corresponds to the saturation pressure (atmospheric pressure for temperatures below 100°C) and the maximum pressure is based on the plant operating experience of hot startups. For the RETRAN-3D dynamic analysis the maximum pressure curve is used. The use of the maximum possible subcooling maximizes the delay in the generation of voids during the CRDA and results in a conservative enthalpy rise calculation. The minimum pressure curve is recommended to be used in the rod mechanical calculations (to be performed in a different project) in order to maximize the cladding differential pressure and to obtain conservative cladding failure criteria.

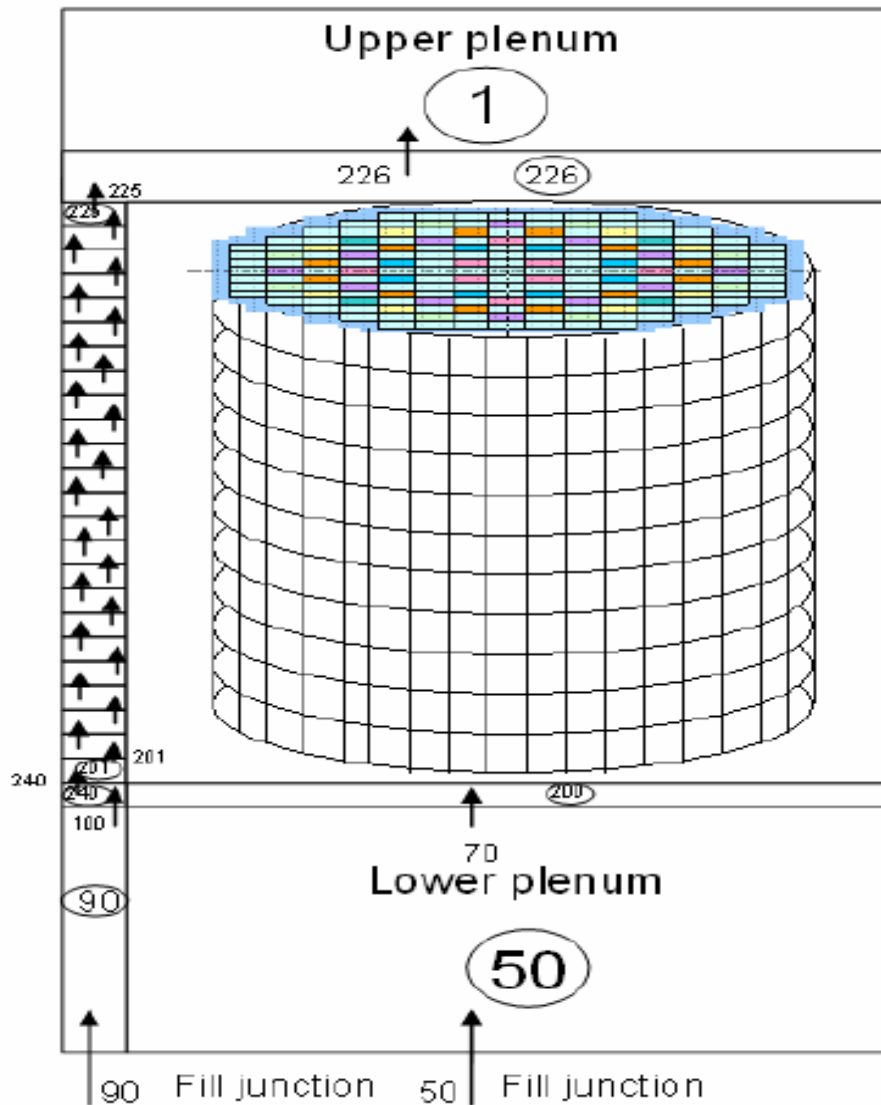


Figure 5-1
CRDA RETRAN Axial Model

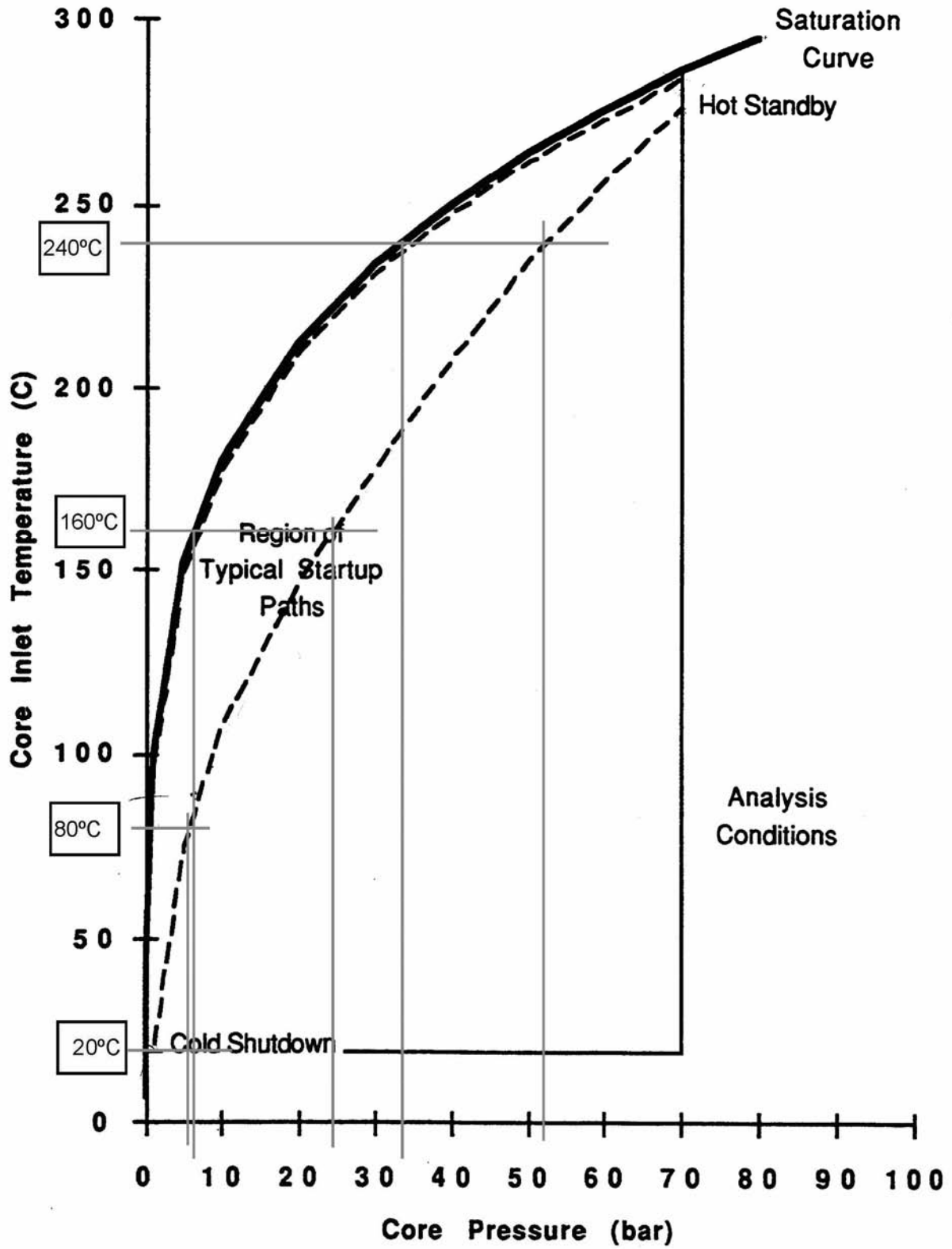


Figure 5-5
Startup Pressure-Temperature Curves

5.2 CRDA Static Comparisons

As indicated in Section 3 of this report, before proceeding with the dynamic analysis a comparison of the static variables obtained in RETRAN-3D and SIMULATE-3 is performed, in order to assure the adequacy of the cross section generation process.

The variables compared are the initial Keff, the beta effective, the power distribution and the rod worth values. For each one of the analysis temperatures (20°C, 80°C, 160°C and 240°C) a comparison of the Keff, beta effective and axial offset is presented in Tables 5-1 to 5-4. The axial power distributions are represented in Figures 5-6 to 5-9. The rod worth comparisons is presented in Table 5-5. As can be seen the comparisons obtained comply with the acceptance criteria indicated in Section 3.

Table 5-1
Static Variables Comparison for 20°C Case

Case 20°C	SIMULATE	RETRAN-3D
Keff	0.95663	0.95437
Beta effective	0.00525	0.00517
Axial Offset	0.99300	0.99351

Table 5-2
Static Variables Comparison for 80°C Case

Case 80°C	SIMULATE	RETRAN-3D
Keff	0.95898	0.95437
Beta effective	0.00524	0.00517
Axial Offset	0.99200	0.99270

Table 5-3
Static Variables Comparison for 160°C

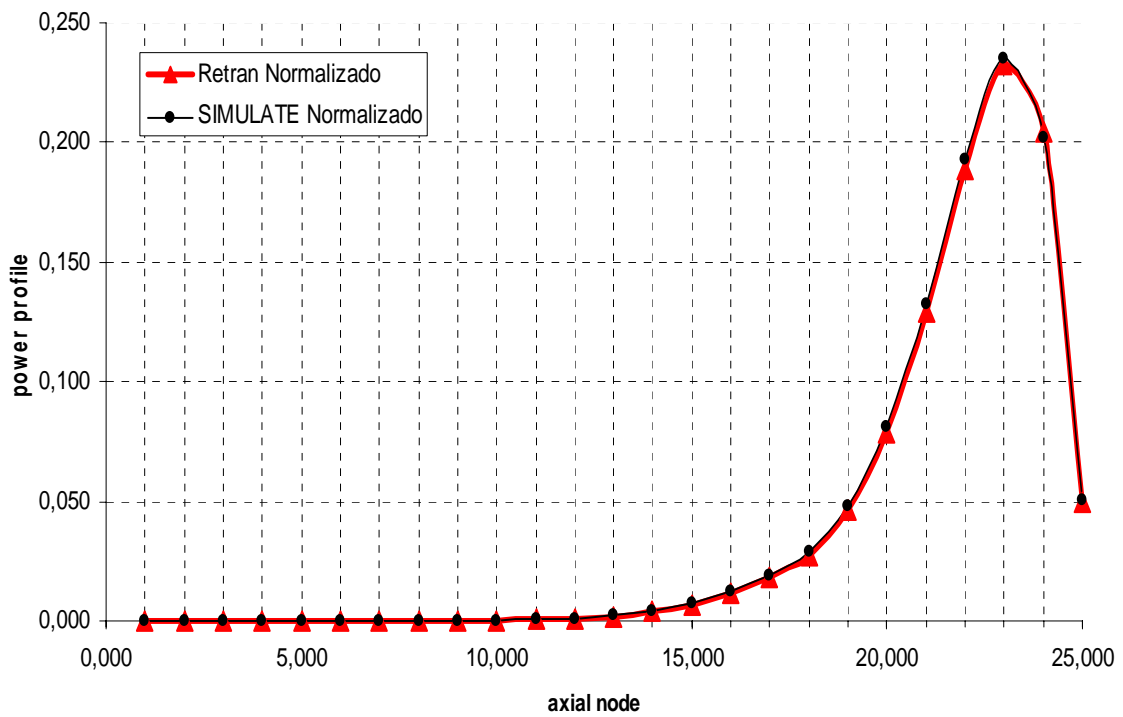
Case 160°C	SIMULATE	RETRAN-3D
Keff	0.96249	0.95642
Beta effective	0.00525	0.00516
Axial Offset	0.98900	0.9899

Table 5-4
Static Variables Comparison for 240°C Case

Case 240°C	SIMULATE	RETRAN-3D
Keff	0.96004	0.95641
Beta effective	0.00522	0.00514
Axial Offset	0.98400	0.98500

**Table 5-5
Rod Worth Comparisons**

Case Temperature	Rod Worth SIMULATE (\$)	Rod Worth RETRAN-3D (\$)
20°C	3.90	4.30
80°C	4.00	4.45
160°C	4.16	4.69
240°C	4.22	4.90



**Figure 5-6
Axial Power Comparison for 20°C Case**

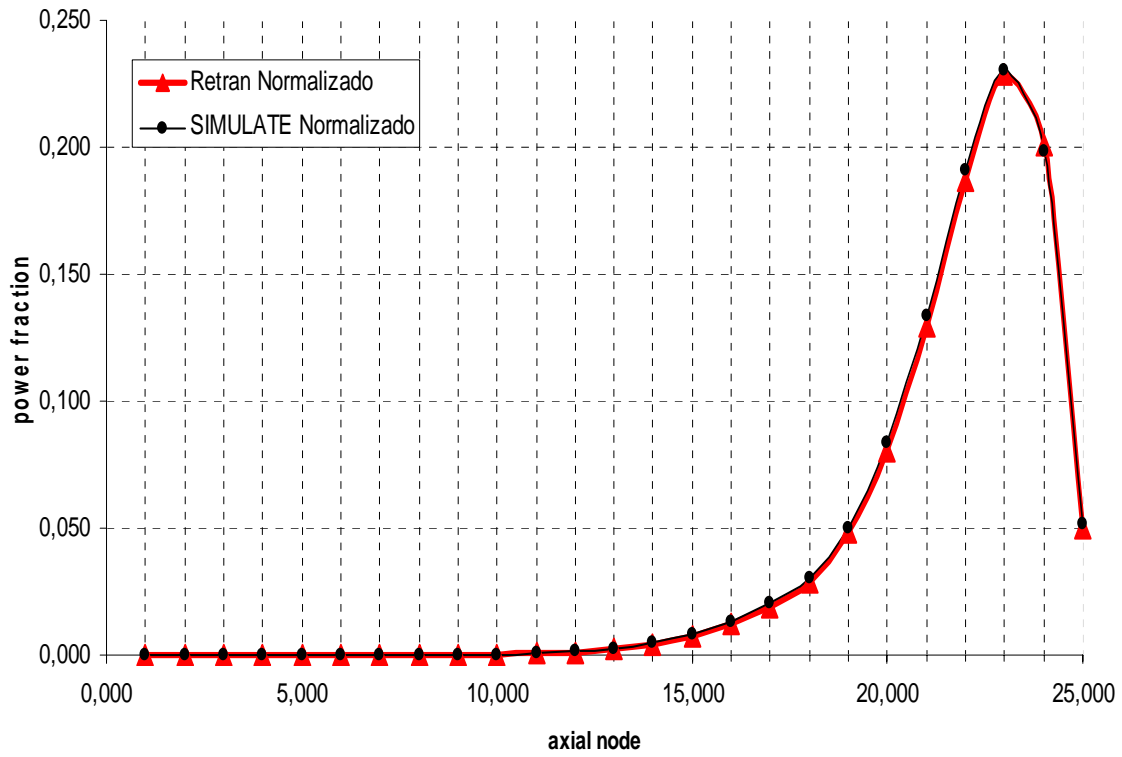


Figure 5-7
Axial Power Comparison for 80°C Case

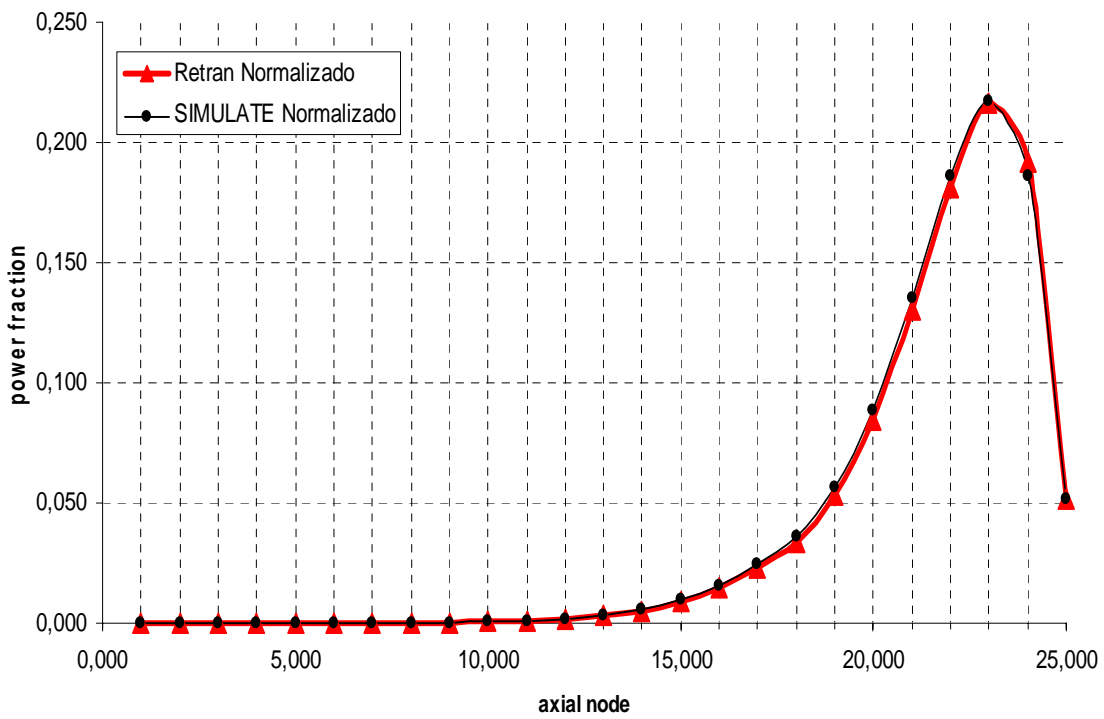


Figure 5-8
Axial Power Comparison for 160°C Case

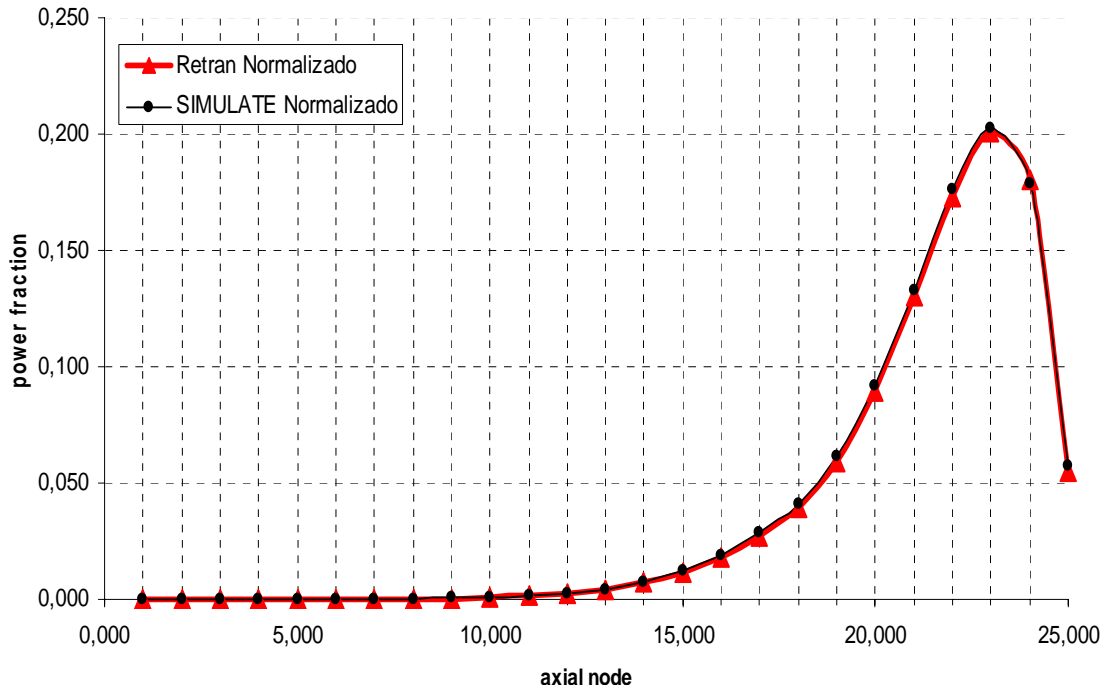


Figure 5-9
Axial Power Comparison for 240°C Case

5.3 Power Results

Once the static results have been verified, a dynamic CRDA analysis is performed for each initial temperature, with the RETRAN model described in Section 5.1.

The evolution of the core power is represented for each case in Figures 5-10 to 5-13.

The results indicate a sharp power increase due to the high dropped rod reactivity that is initially stopped by the Doppler coefficient. After the initial power reduction, a clear power tail is calculated for the cases with significant initial subcooling (cases of 20, 80 and 160 °C). For these cases the power is finally decreased when the scram rods are inserted (beyond 3 seconds). For the low subcooling case (240°C case) the generation of voids is significant before the scram insertion and therefore the reactor power is finished by the void reactivity feedback. This results in a negligible power tail for this case. The significance of this will be discussed in the following sections.

A more detail representation of the power peaks is illustrated in Figure 5-14. The typical cosine forms are clearly observed. The first power peak is also observed to increase with the rod worth value. In this way the hot case (240°C) has a higher power peak than the cold case (20°C) due to the higher rod worth value obtained for the hot case (see Table 5-5). This higher power peak does not imply a higher enthalpy as will be seen in the next section, due to the significant contribution of the power tail to the total fuel enthalpy.

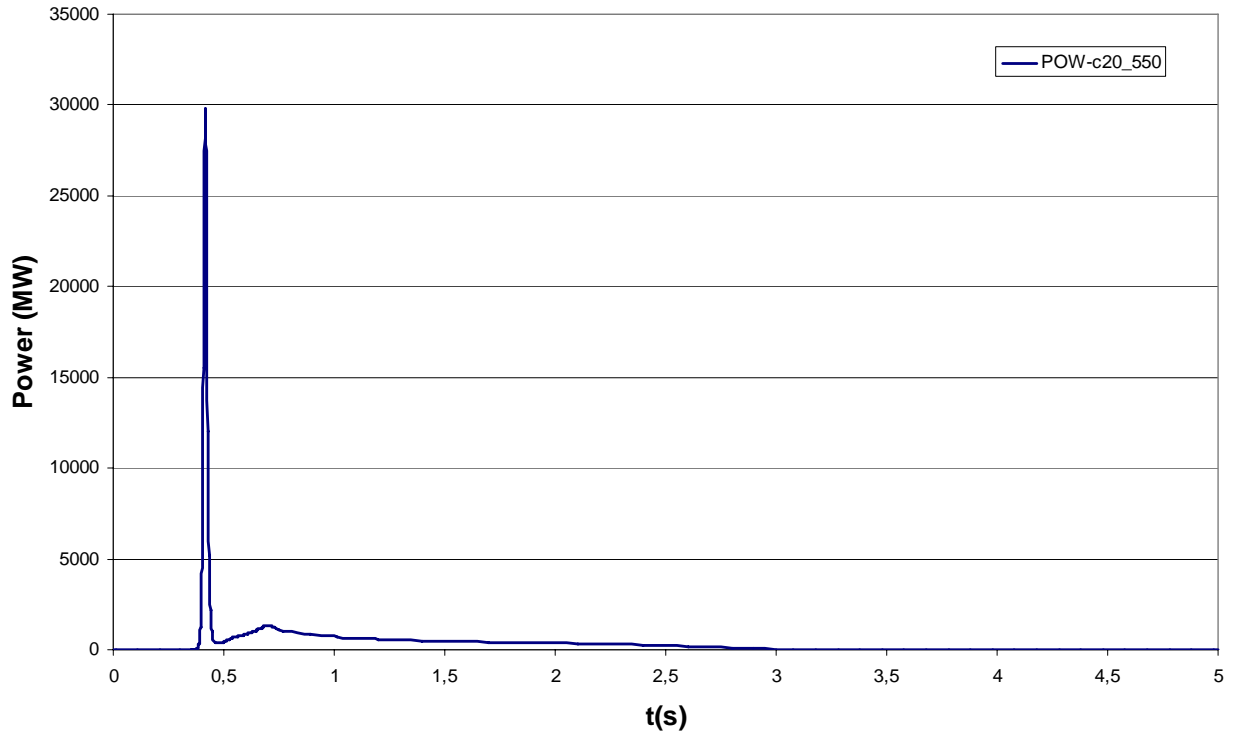


Figure 5-10
Core Power Evolution for the 20°C Case

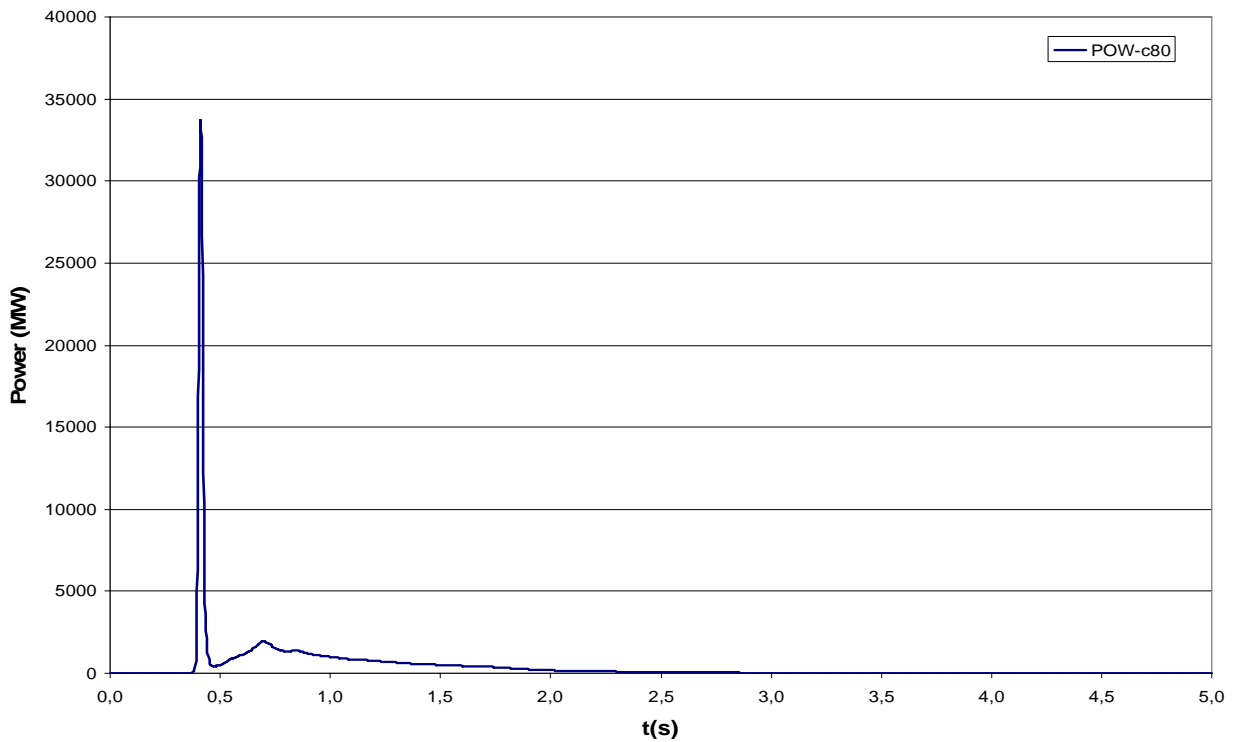


Figure 5-11
Core Power Evolution for the 80°C Case

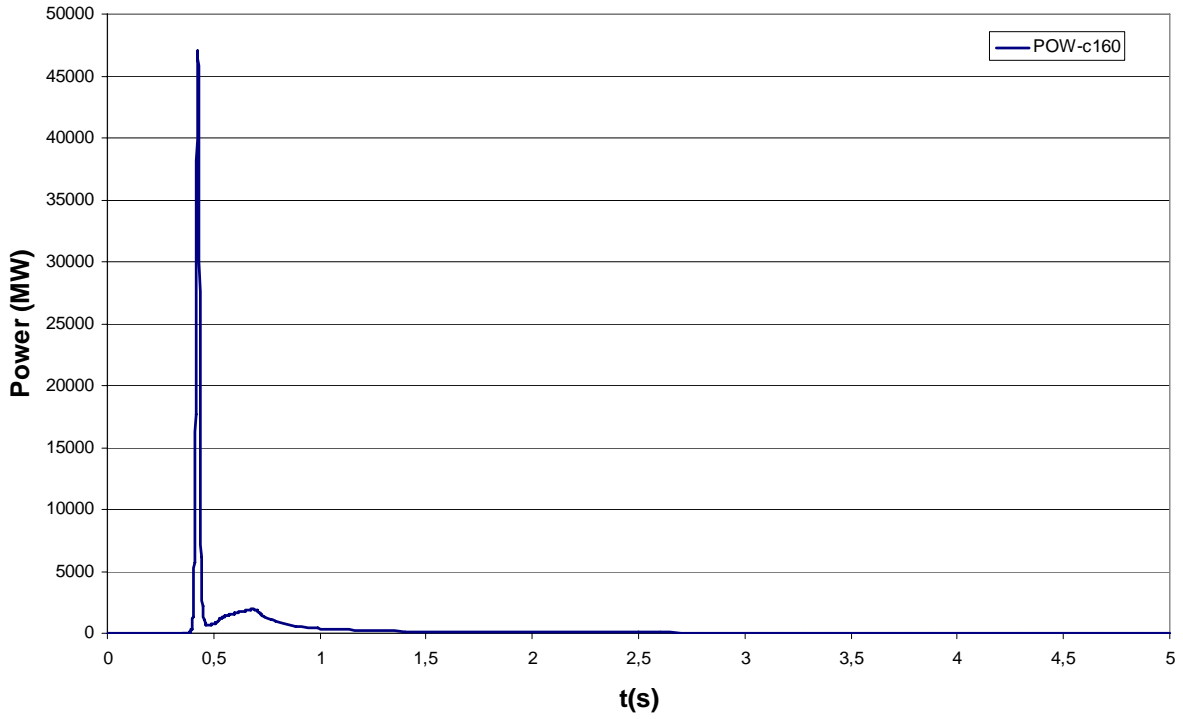


Figure 5-12
Core Power Evolution for the 160°C Case

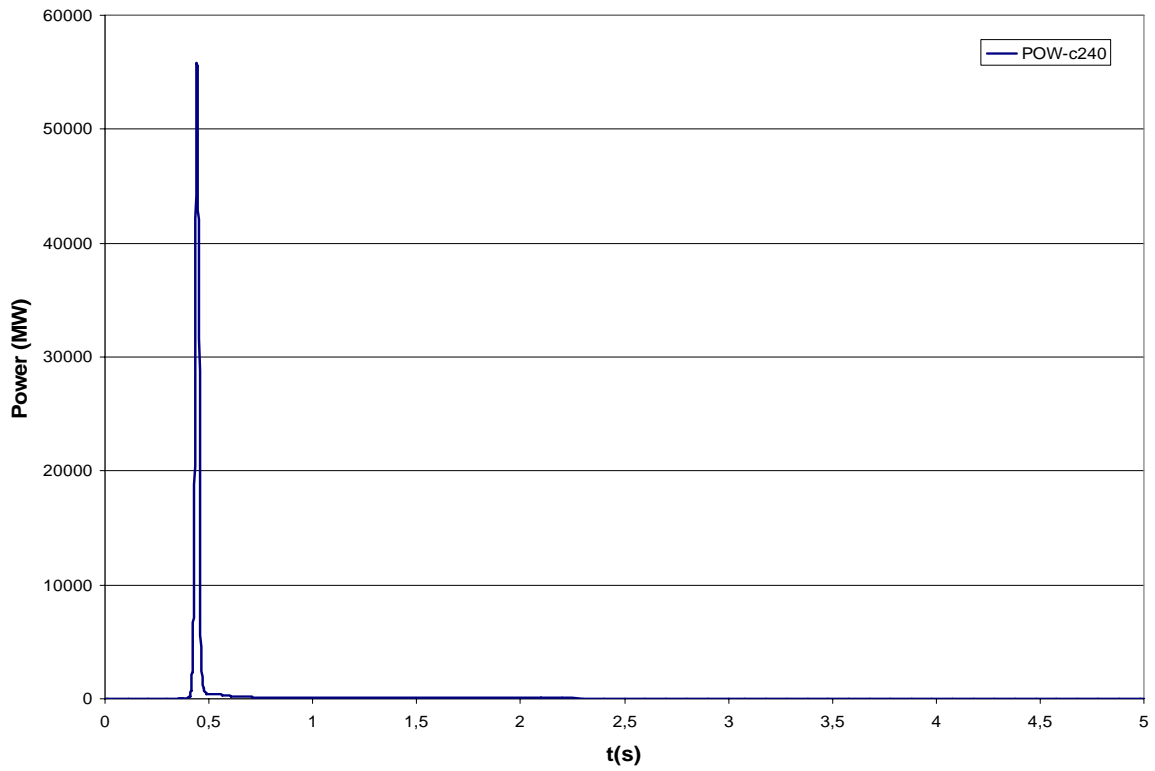


Figure 5-13
Core Power Evolution for 240°C Case

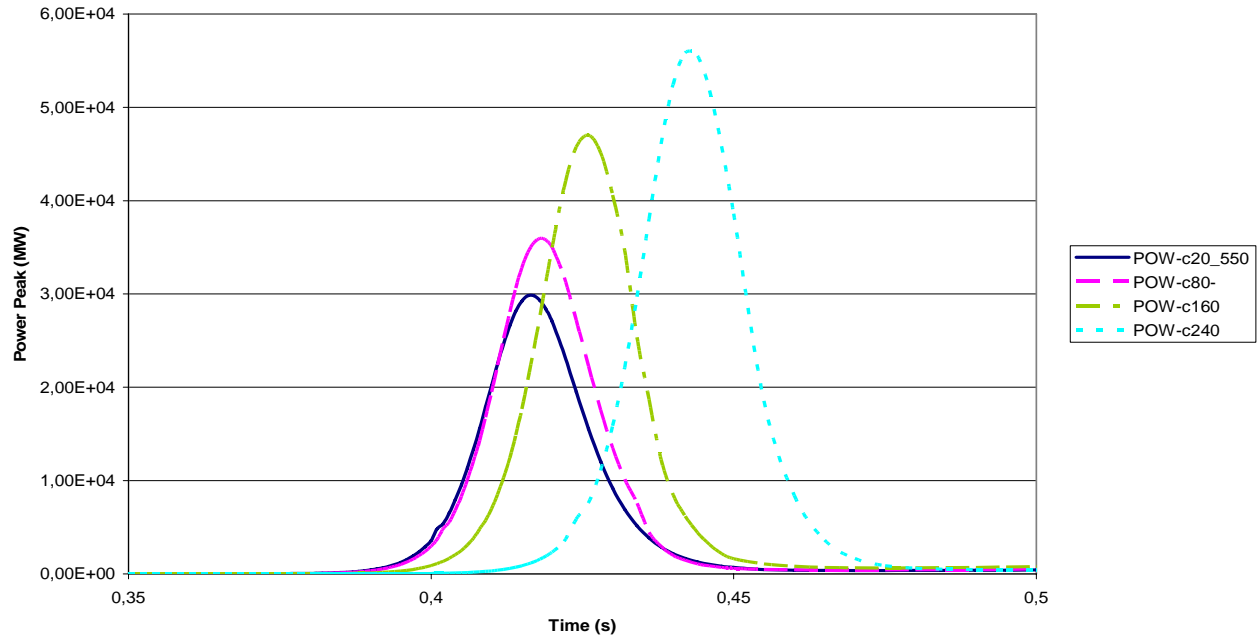


Figure 5-14
Detailed Peak Power Curves

5.4 Enthalpy Results

Based on the power results the corresponding enthalpy evolution as calculated by RETRAN-3D, is obtained. Detailed information is available for the 16 bundles surrounding the dropped rod location. The bundle burnups and their corresponding plant and RETRAN coordinates are represented in Figure 5-15.

For each one of analyzed cases, and in order to perform additional thermomechanical calculations, detailed information of the RETRAN-3D power axial evolution and thermohydraulic boundary conditions has been provided for six selected bundles around the dropped rod. The six chosen bundles are highlighted in Figure 5-15. They are selected to span the range of burnups available and close to the dropped rod in order to get as much enthalpy rise as possible. These bundles will be analyzed with FALCON in a separate project in order to determine their thermomechanical behavior and the impact on the CRDA failure limits.

The enthalpy evolution obtained in the 20°C case for each one of the bundles surrounding the drop rod is presented in Figure 5-16. It can be seen that after an initial enthalpy rise due to the power peak (prompt enthalpy) there is a significant enthalpy rise due to the delayed power tail.

The total enthalpy rise for the different bundle exposures is represented in Figures 5-17 and 5-18. It can be seen that there is no direct relationship between the bundle burnup and the total enthalpy rise, and that the proximity of the bundle to the dropped rod has an important effect. From these results it also can be seen that high burnup bundles located adjacent to the dropped rod can have enthalpy rise values similar to those obtained for the limiting bundles (with lower burnups).

Plant Coordinates	21	23	25	27	
52	25.5	27.2	28	28.3	4
50	49.3	30.8	52.2	30.9	5
48	32.1	54.2	32.8	54.7	6
46	54.1	33	54.7	32.9	7
	12	13	14	15	Code coordinates

Figure 5-15
Bundle Exposures (GWd/MT) Around the Dropped Rod

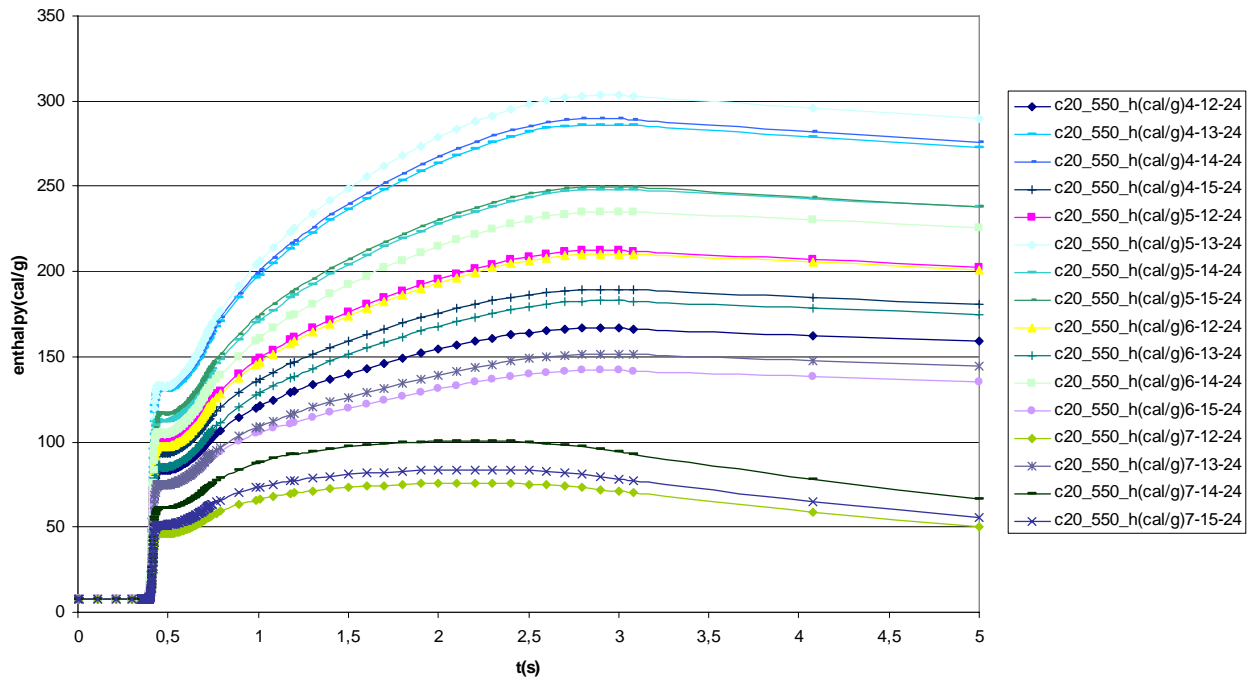


Figure 5-16
Enthalpy vs. Time for the 20°C Case

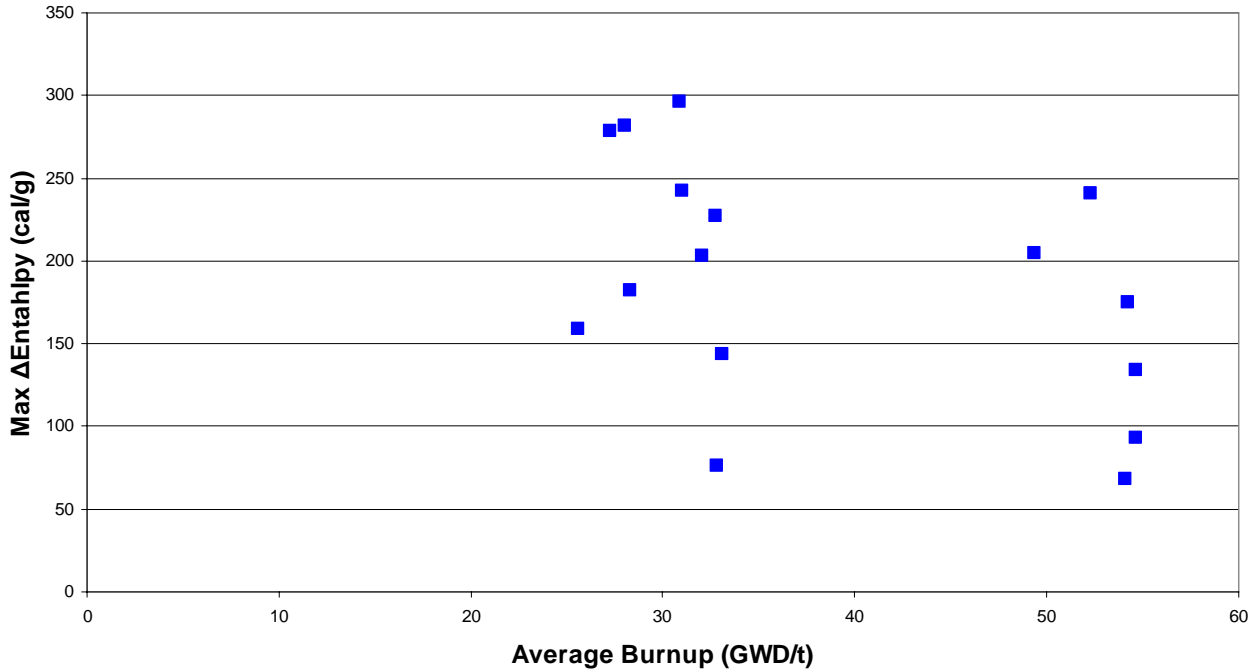


Figure 5-17
Enthalpy Rise vs. Burnup for the 20°C Case

Plant Coordinates	21	23	25	27	
52	159.21	278.66	282.01	181.94	4
50	204.82	295.99	240.69	242.29	5
48	202.70	175.28	227.33	134.40	6
46	68.24	144.01	92.91	76.11	7
	12	13	14	15	Code Coordinates

Figure 5-18
Enthalpy Rise (cal/g) for Each Bundle in the 20°C Case

Similar results are obtained for the 80°C case (see Figures 5-19, 5-20 and 5-21). For the 160°C case a reduction in the total enthalpy rise is observed (Figures 5-22, 5-23 and 5-24) and for the 240°C case the total enthalpy rise coincides with the prompt enthalpy rise since there is no power tail to increase the enthalpy after the peak power has passed (Figures 5-25, 5-26 and 5-27).

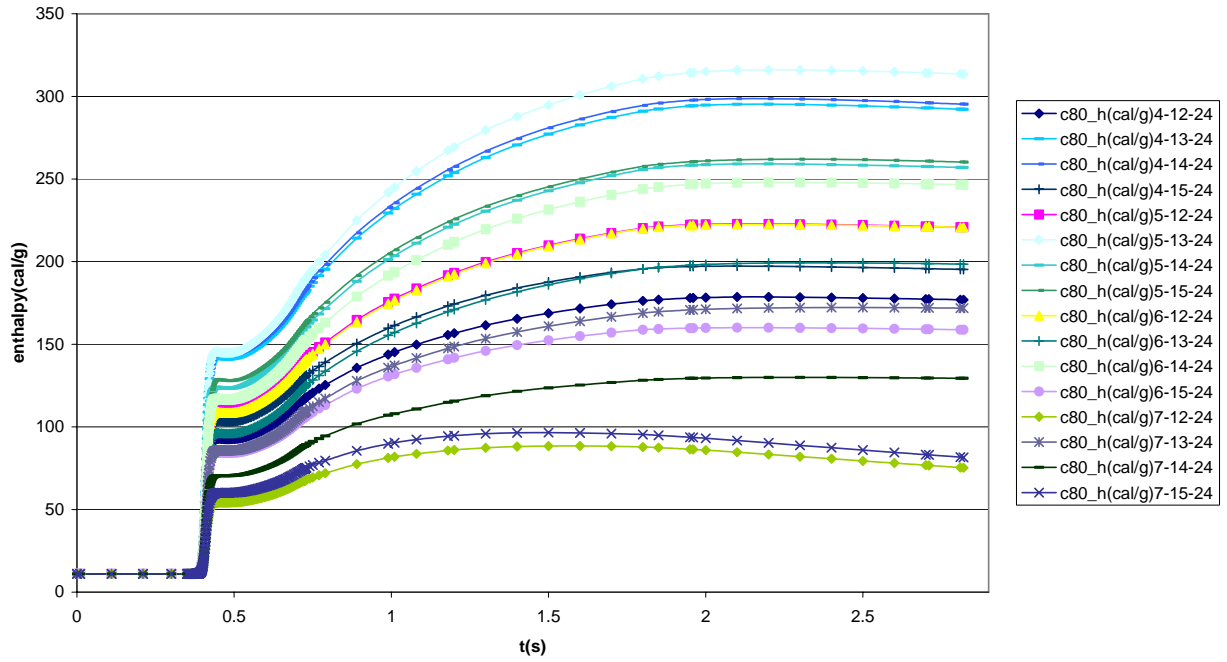


Figure 5-19
Enthalpy vs. Time for the 80°C Case

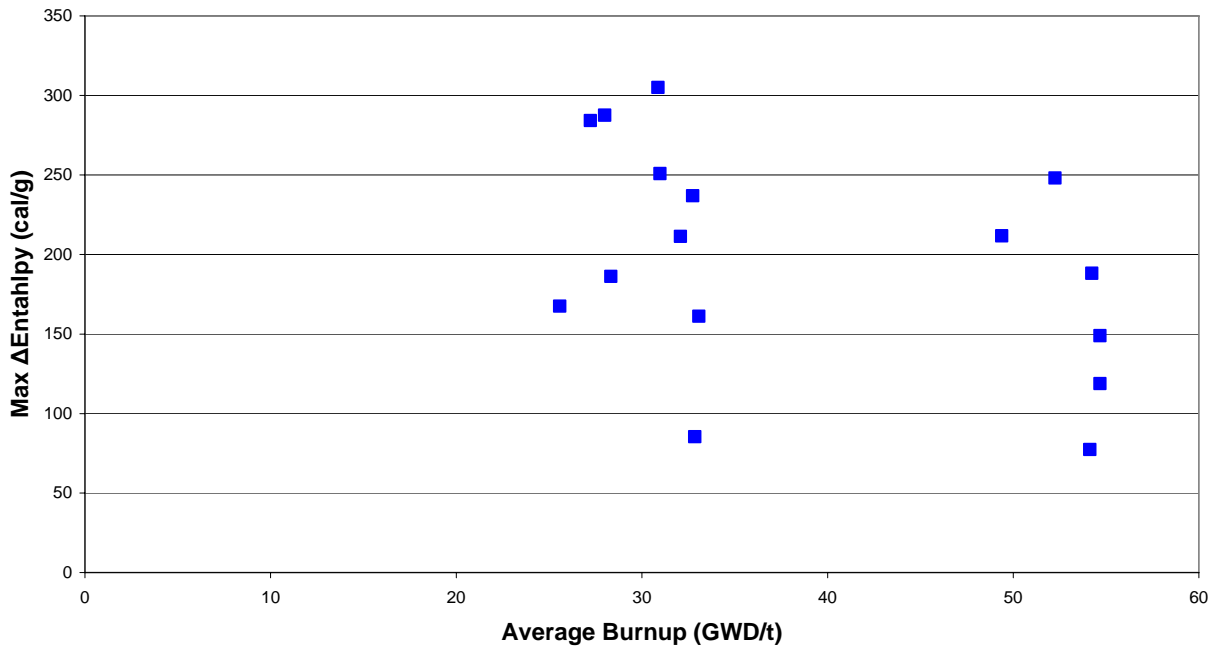


Figure 5-20
Enthalpy Rise vs. Burnup for the 80°C Case

Plant Coordinates	21	23	25	27	
52	167.58	284.27	287.60	186.27	4
50	211.80	305.09	248.13	250.94	5
48	211.47	188.23	236.97	149.00	6
46	77.38	161.18	118.87	85.49	7
	12	13	14	15	Code Coordinates

Figure 5-21
Enthalpy Rise (cal/g) for Each Bundle in the 80°C Case

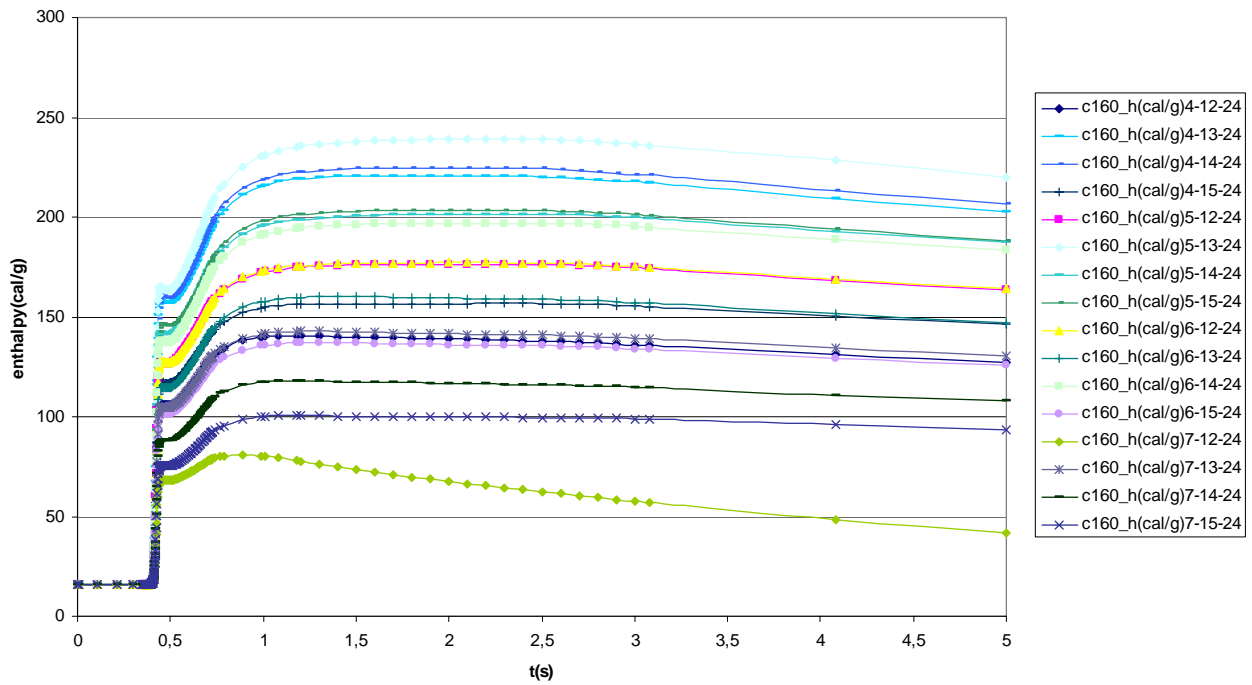


Figure 5-22
Enthalpy vs. Time for the 160°C Case

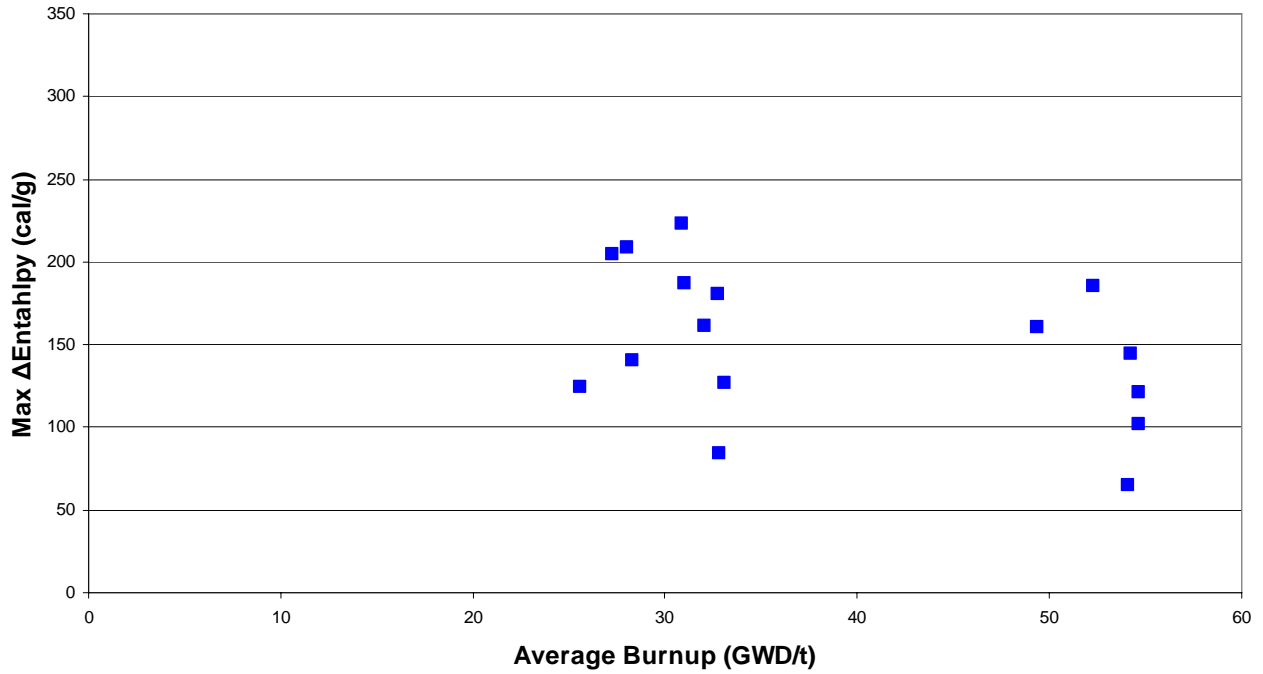


Figure 5-23
Enthalpy Rise vs. Burnup for the 160°C Case

Plant Coordinates	21	23	25	27	
52	124.31	204.75	208.74	140.57	4
50	160.32	222.82	185.52	187.24	5
48	161.08	144.24	180.82	121.00	6
46	64.81	126.72	101.62	84.43	7
	12	13	14	15	Code Coordinates

Figure 5-24
Enthalpy Rise (cal/g) for Each Bundle in the 160°C Case

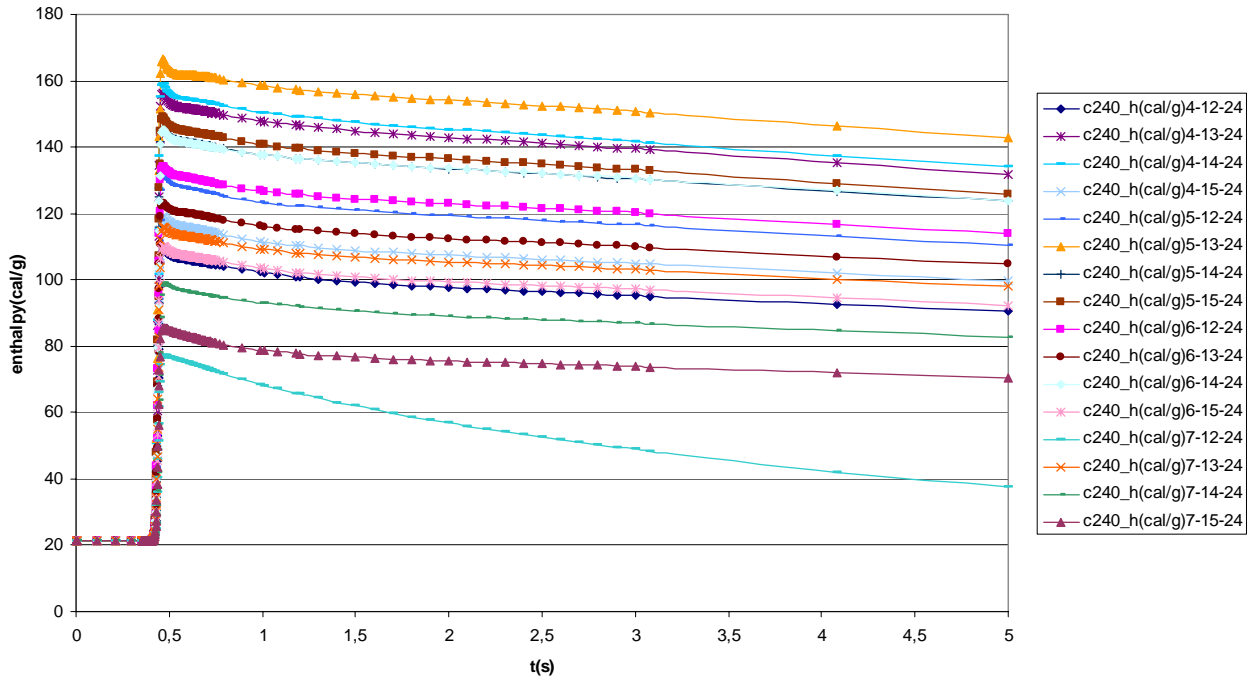


Figure 5-25
Enthalpy vs. Time for the 240°C Case

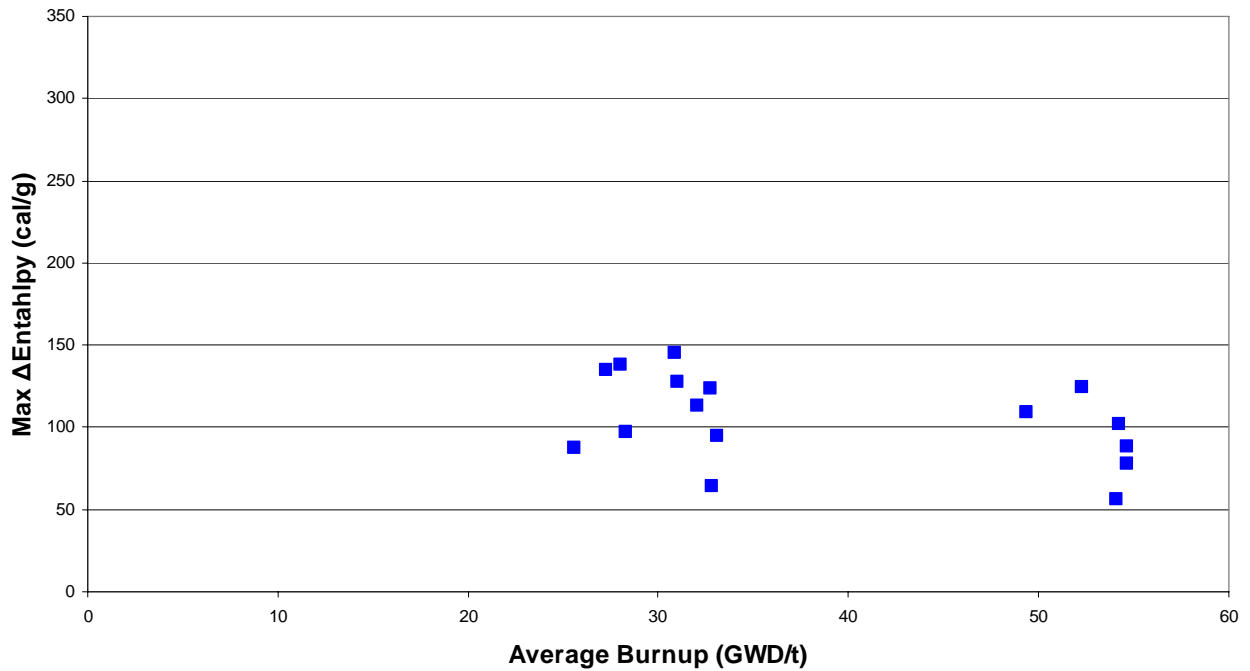


Figure 5-26
Enthalpy Rise vs. Burnup for the 240°C Case

Plant Coordinates	21	23	25	27	
52	87.49	134.95	137.77	97.51	4
50	109.49	145.01	124.24	127.68	5
48	112.84	101.58	123.89	88.59	6
46	55.93	94.46	77.52	64.20	7
	12	13	14	15	Code Coordinates

Figure 5-27
Enthalpy Rise (cal/g) for Each Bundle in the 240°C Case

5.5 PCMI Failure Considerations

The results obtained in the CRDA dynamic analysis indicate that for the cases with a significant initial subcooling, an important part of the total enthalpy rise during the accident is due to the existence of a power tail. This effect can be clearly seen in the plots showing the evolution of the fuel enthalpy. A fast initial enthalpy rise is observed due to the power peak. A prompt enthalpy (enthalpy at the time of the peak power plus one pulse width) is defined to quantify this effect. During this period of time the cladding temperatures are close to their initial values (see Section 5.6 of this report).

After the fast initial enthalpy increase there is a slower enthalpy rise due to the delayed power tail. During this period the cladding temperatures increase significantly (see Section 5.6).

The ratio between the prompt enthalpy rise and the total enthalpy rise for the limiting bundles around the drop rod is represented in Figure 5-28 and Table 5-6.

Table 5-6
Enthalpy Ratio as Function of Initial Subcooling

Case Temperature	Initial Subcooling (°C)	Ratio Prompt/Total Enthalpy Rise
20°C	100	0.44
80°C	99	0.46
160°C	62	0.67
240°C	24	1.00

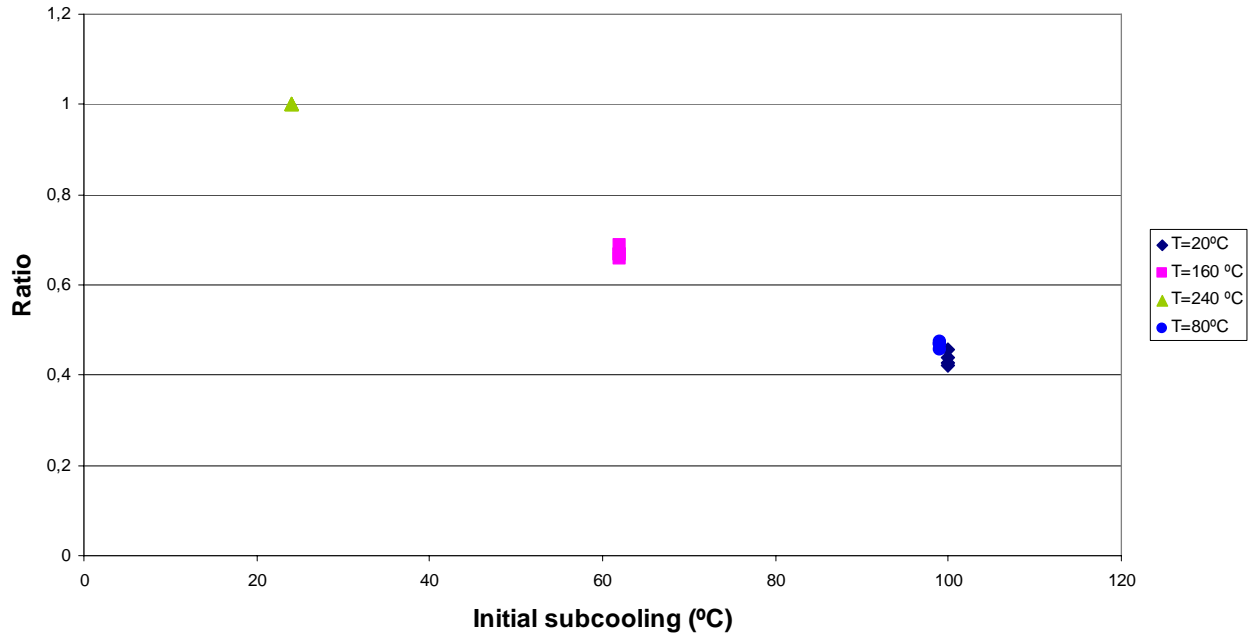


Figure 5-28
Ratio of Enthalpies as Function of Subcooling

In Figures 5-29 and 5-30 the enthalpy ratio is represented as function of the bundle burnup and the total enthalpy rise. No clear dependency on these variables is observed. A clear impact of the initial subcooling is however observed in Figure 5-28 and Figure 5-31. In this last figure the prompt enthalpy and the total enthalpy values for all the bundles surrounding the drop rod are represented vs. the initial subcooling. It can be clearly observed that the maximum prompt enthalpy decreases slowly with the initial subcooling (slightly lower rod worth value) but the maximum total enthalpy increases significantly with the initial subcooling.

The significance of the prompt enthalpy and the total enthalpy in the potential cladding failure due to Pellet Cladding Mechanical Interaction (PCMI) will be studied in a separate EPRI project.

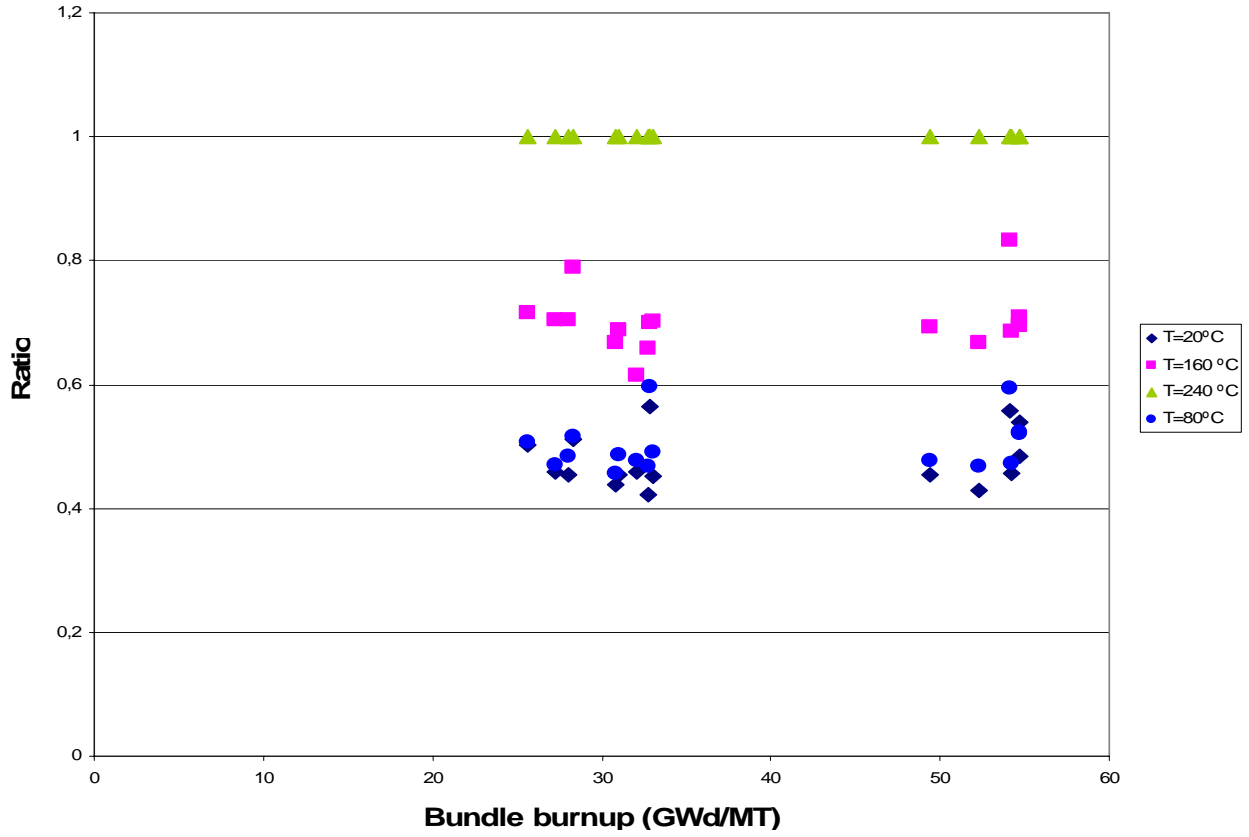


Figure 5-29
Enthalpy Ratio vs. Bundle Burnup

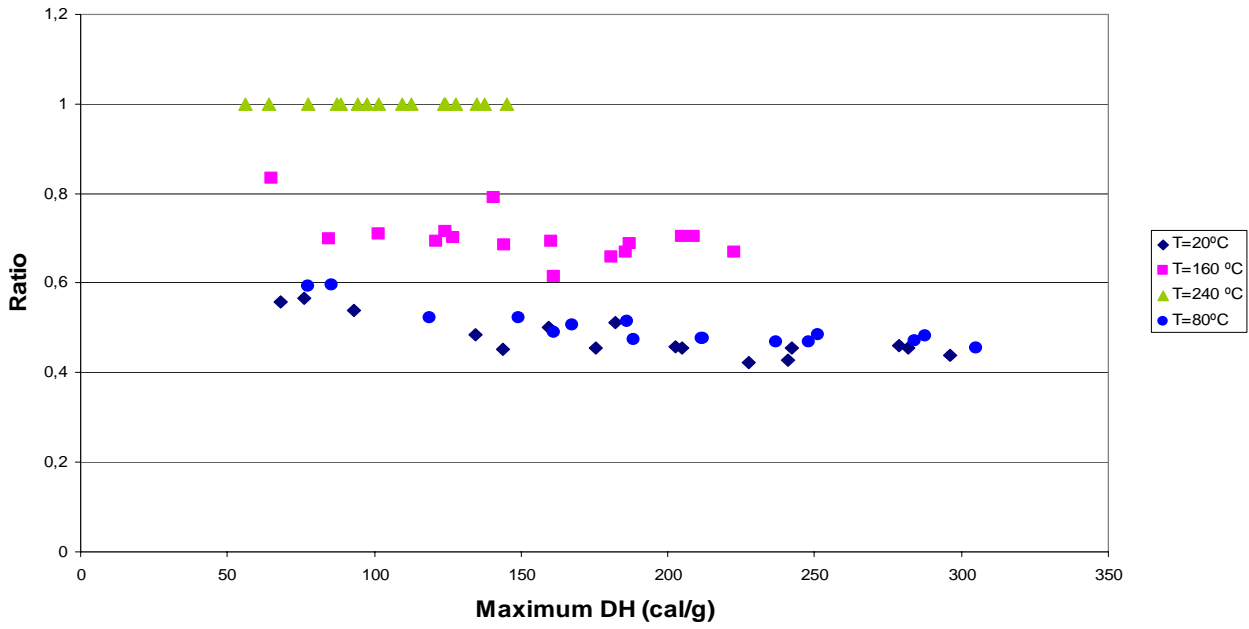


Figure 5-30
Enthalpy Ratio vs. Maximum Enthalpy Rise

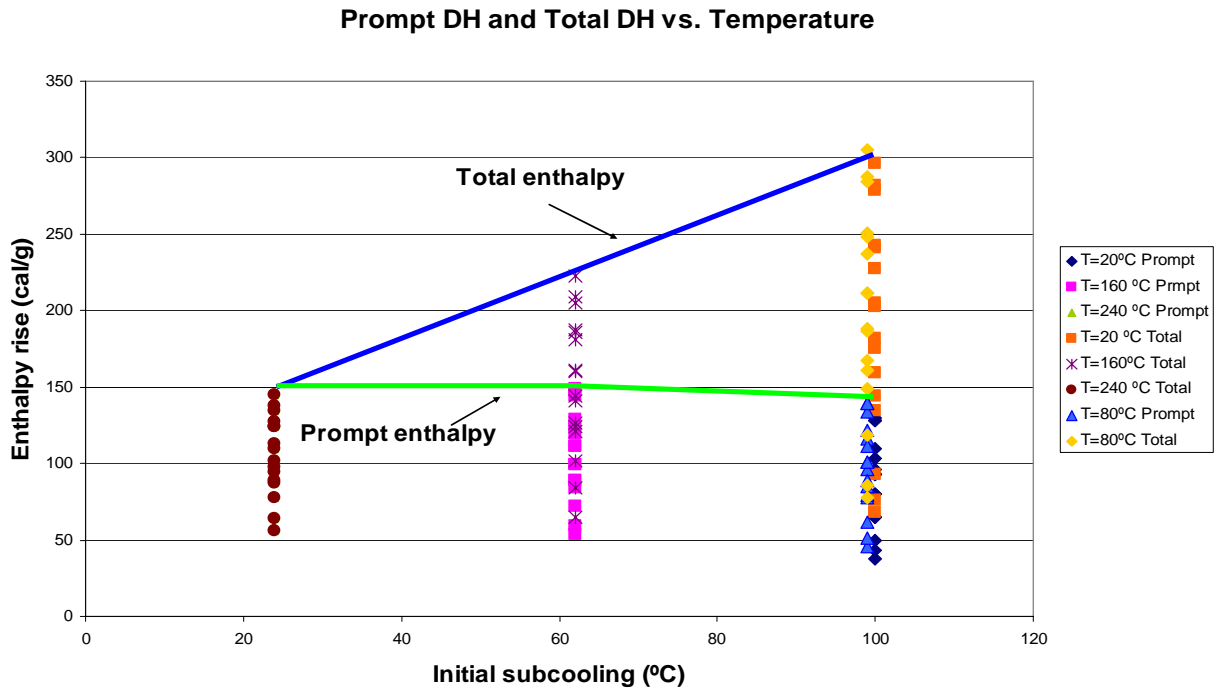


Figure 5-31
Prompt and Total Enthalpy vs. Initial Subcooling

5.6 DNB Failure Considerations

The typical temporal evolution of the cladding temperature with respect to the fuel enthalpy during the CRDA can be observed in the Figure 5-32. It can be seen that the prompt enthalpy rise is produced in a short time period and the cladding temperatures do not increase significantly during this period. This is due to the time needed to transfer the deposited energy from the fuel to the cladding. After that the delayed enthalpy rise occurs at a slower rate and the cladding temperatures follow the total enthalpy rise.

The maximum cladding temperature (PCT) is therefore, function of the total enthalpy rise. The relationship between the PCT and the total enthalpy rise is observed in Figure 5-33 for the different bundles and at the different initial temperatures. It can be seen that the enthalpy at which the cladding temperature starts to increase (departure from nucleate boiling-DNB enthalpy) is higher when the initial subcooling is higher. However the maximum cladding temperatures reached are relatively independent of the initial subcooling and strongly dependent on the total enthalpy. Only the cases with PCT below the cladding melting temperature (2000°C) are shown in Figure 5-33.

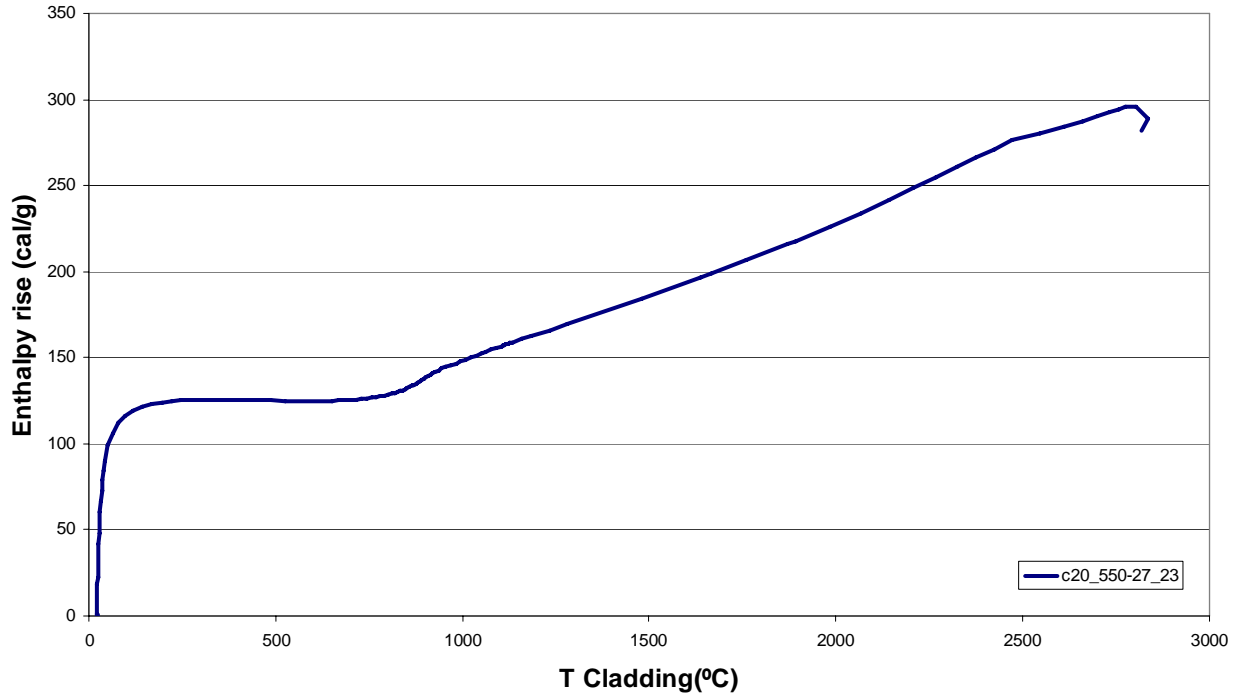


Figure 5-32
Evolution of Cladding Temperature vs. Enthalpy Rise for the limiting Bundle in the 20°C Case

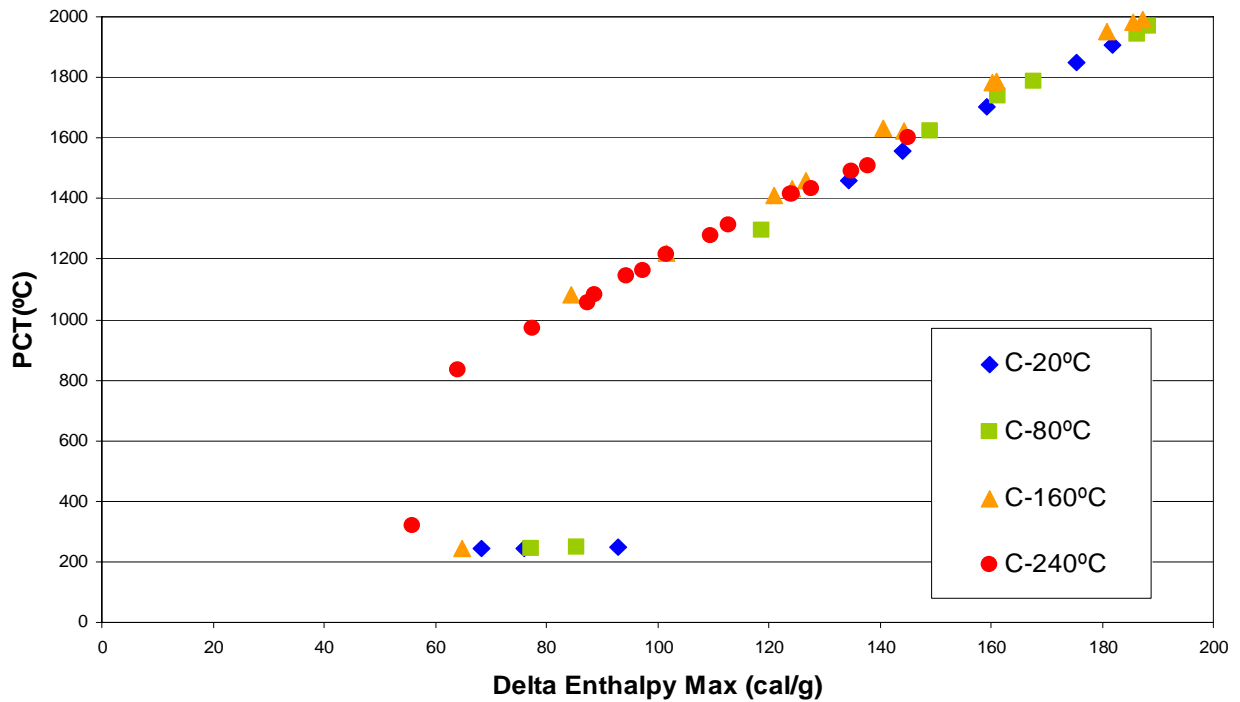


Figure 5-33
Cladding PCT vs. Total Enthalpy Rise for the Different Initial Temperatures

To verify the adequacy of the RETRAN models in the determination of the DNB phenomenon at CRDA conditions, a comparison with CDC-SPERT and Japanese-NSRR experiments has been made. Experiments with similar initial temperatures (20°C) and rod geometry have been selected from the literature [12]. Rods with a ratio of initial gap width to pellet radius similar to the SVEA-96-OPTIMA 2 fuel rod have been selected (GEP rods in CDC and standard and JPDR-II rods in NSRR). This ratio determines the enthalpy needed to close the gap between the fuel pellet and the cladding and therefore the initiation of the DNB phenomenon. The results are presented in Figure 5-34 and indicate a good coincidence in the enthalpies needed to initiate DNB between RETRAN calculations and experimental results.

Incipient DNB is obtained for relative low values of enthalpy rise (100-140 cal/g for 20°C initial temperature, 60-80 cal/g for 240°C initial temperature). The relevance of the DNB phenomenon on the cladding failure due to ballooning and rupture will be determined in a separate EPRI project.

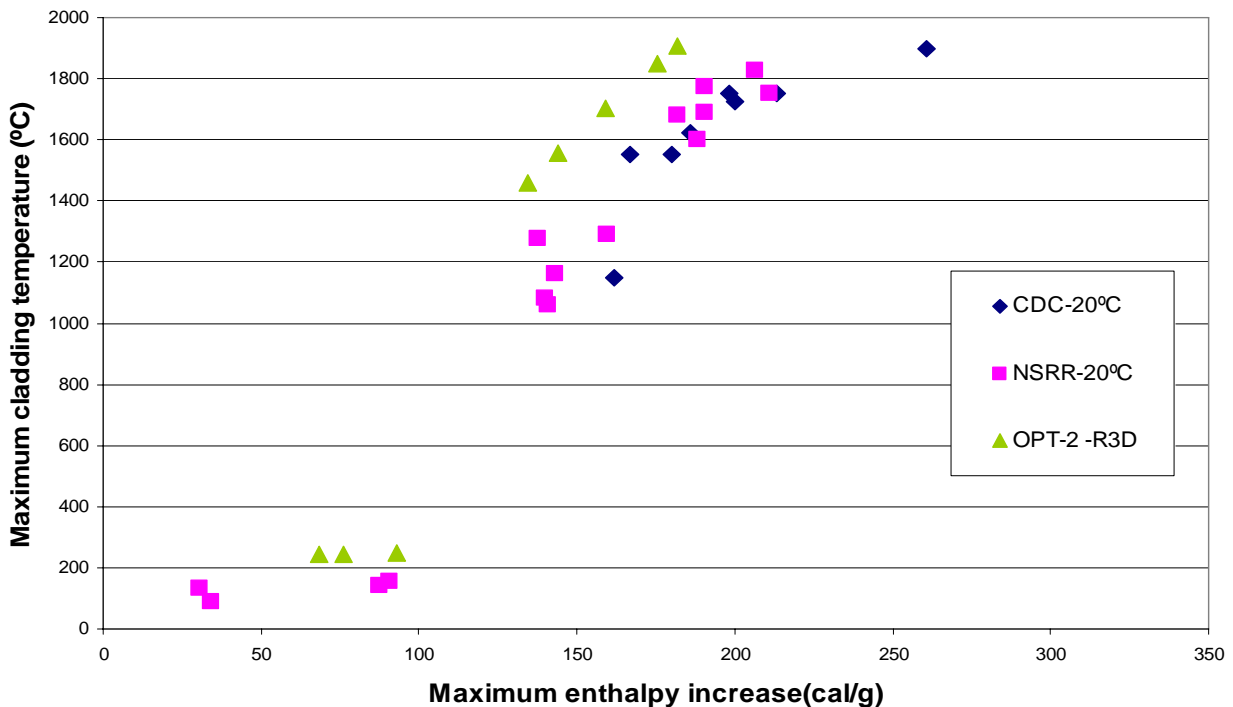


Figure 5-34
RETRAN DNB Prediction and Comparison with Experiments

6

CONCLUSIONS

Detailed 3D kinetic analyses have been performed with the RETRAN-3D code for different initial temperatures expected at a BWR CRDA during the plant startup process.

Cases with a significant initial subcooling present a significant power tail well after the power peak has passed. For these cases the power is not reduced until the scram rods are inserted. This power tail produces a significant delayed enthalpy rise.

The ratio between the prompt enthalpy rise and the total enthalpy rise is established as figure of merit to differentiate the different behavior during CRDA. This ratio is strongly dependent on the initial subcooling (the higher the subcooling the lower the ratio), but is independent on the fuel burnup or the total enthalpy rise.

During the prompt enthalpy rise the cladding temperature remains relatively invariant and equal to the initial temperature. During the delayed enthalpy rise the cladding temperatures increase significantly increasing the cladding ductility.

The phenomenon of DNB has been calculated to occur at relatively low enthalpy rise values, especially for the high temperature case. The significance of these results on the cladding failure due to ballooning and rupture will be determined in a separate EPRI project.

7

REFERENCES

1. NUREG-800, "USNRC Standard Review Plan", Office of Nuclear Reactor Regulation, Section 15.4.9, Spectrum of Rod Drop Accidents (BWR), Revision 2 July 1981.
2. "Research Information Letter No 0401, An Assessment of Postulated Reactivity-Initiated Accidents for Operating Reactors in the U.S., March 31 2004
3. "RETRAN-3D: A Program for Transient Thermal-Hydraulic Analysis of Complex Fluid Flow Systems", Electric Power Research Institute, Palo Alto, CA, EPRI-NP 7450, October 1996.
4. "SIMULATE-3: Advanced Three-Dimensional Two-Group Reactor Analysis Code", Studsvik/SOA-95/15 Rev. 0, October 1995.
5. Andres J. Gomez et al. "Validation of SIMTAB Cross Sections Generator Method for TRAC-NEM from SIMULATE-3", 2004 TUG Meeting, Gostport, May 2004.
6. Safety Evaluation by the Office of Nuclear Reactor Regulation Related to EPRI-NP-7450(P) "RETRAN-3D- A Program for Transient Thermal-Hydraulic of Complex Fluid Systems" EPRI Project No 669, January 25 2001.
7. Andres J. Gomez et al. "Analysis of a Reactivity Initiated Accident (RIA) in Cofrentes NPP, Cold and Hot Conditions with RETRAN-3D", 2005 Water Reactor Fuel Performance Meeting, Kyoto, Japan, October 2-6 2005.
8. Javier Riverola et al. "Realistic and Conservative Rod Ejection Simulation in a PWR Core at HZP, EOC, with Coupled PARCS and RELAP", Proceedings of the 2004 International Meeting on LWR Fuel Performance, Orlando Florida, September 19-22, 2004.
9. CENPD-284-P-A "Control Rod Drop Accident Analysis Methodology for Boiling Water Reactors: Summary and Qualification", ABB Combustion Engineering Nuclear Operations, July 1996.
10. IT-COSNU-205 "Methodology for the Licensing Analysis of Control Rod Drop Accident (CRDA) for Cofrentes NPP. Control Rod Calculations, Rev.0 March 2004.
11. NEDO 21231 "Banked Position Withdrawal Sequence", C. J. Paone, January 1977.
12. NUREG/CR-0269, TREE-1237, "Light Water Reactor Fuel Response During Reactivity Initiated Accident Experiments", August 1978.



WARNING: This Document contains information classified under U.S. Export Control regulations as restricted from export outside the United States. You are under an obligation to ensure that you have a legal right to obtain access to this information and to ensure that you obtain an export license prior to any re-export of this information. Special restrictions apply to access by anyone that is not a United States citizen or a permanent United States resident. For further information regarding your obligations, please see the information contained below in the section titled "Export Control Restrictions."

Export Control Restrictions

Access to and use of EPRI Intellectual Property is granted with the specific understanding and requirement that responsibility for ensuring full compliance with all applicable U.S. and foreign export laws and regulations is being undertaken by you and your company. This includes an obligation to ensure that any individual receiving access hereunder who is not a U.S. citizen or permanent U.S. resident is permitted access under applicable U.S. and foreign export laws and regulations. In the event you are uncertain whether you or your company may lawfully obtain access to this EPRI Intellectual Property, you acknowledge that it is your obligation to consult with your company's legal counsel to determine whether this access is lawful. Although EPRI may make available on a case-by-case basis an informal assessment of the applicable U.S. export classification for specific EPRI Intellectual Property, you and your company acknowledge that this assessment is solely for informational purposes and not for reliance purposes. You and your company acknowledge that it is still the obligation of you and your company to make your own assessment of the applicable U.S. export classification and ensure compliance accordingly. You and your company understand and acknowledge your obligations to make a prompt report to EPRI and the appropriate authorities regarding any access to or use of EPRI Intellectual Property hereunder that may be in violation of applicable U.S. or foreign export laws or regulations.

The Electric Power Research Institute (EPRI), with major locations in Palo Alto, California, and Charlotte, North Carolina, was established in 1973 as an independent, nonprofit center for public interest energy and environmental research. EPRI brings together members, participants, the Institute's scientists and engineers, and other leading experts to work collaboratively on solutions to the challenges of electric power. These solutions span nearly every area of electricity generation, delivery, and use, including health, safety, and environment. EPRI's members represent over 90% of the electricity generated in the United States. International participation represents nearly 15% of EPRI's total research, development, and demonstration program.

Together...Shaping the Future of Electricity

Program:

Nuclear Power

© 2007 Electric Power Research Institute (EPRI), Inc. All rights reserved. Electric Power Research Institute, EPRI, and TOGETHER...SHAPING THE FUTURE OF ELECTRICITY are registered service marks of the Electric Power Research Institute, Inc.

Printed on recycled paper in the United States of America

1015206

Electric Power Research Institute

3420 Hillview Avenue, Palo Alto, California 94304-1338 • PO Box 10412, Palo Alto, California 94303-0813 USA
800.313.3774 • 650.855.2121 • askepri@epri.com • www.epri.com